Comparative Study of Semi-analytical and Numerical Methods for Solving Falkner-Skan Equations

Yannick Harisson NKOCKO AWOUNTSA (yannick@aims.ac.za)
African Institute for Mathematical Sciences (AIMS)

Supervised by: Prof. Precious Sibanda
University of KwaZulu-Natal, South Africa

Co-supervised by: Dr. Sicelo Goqo
University of KwaZulu-Natal, South Africa

24 October 2019

Submitted in partial fulfillment of a structured masters degree at AIMS South Africa

Abstract

We present a comparative study of the solution of Falkner-Skan equations (a third-order boundary value problem arising in boundary-layer theory) using semi-analytical and numerical methods. Physical quantities such as the skin friction, shear stress and displacement are also studied depending on the dimensionless pressure gradient parameter β. Numerical methods used include the so-called spectral quasi-linearisation method (SQLM) and the Matlab function ODE45. The homotopy analysis method (HAM) is used as an example of a semi-analytical method. To our knowledge, it is the first time the spectral quasi-linearisation method is used to solve the Falner-Skan equations and the comparison between the HAM, SQLM and the ODE45 is given to compare the accuracy and the efficiency of semi-analytical and numerical methods. The result shows that the number of iterations before converging to the solution is 4 for SQLM followed by 7 for ODE45 and the 20th order approximation for HAM. We observe that the iterative error after 3 iterations for SQLM is 10^{-7} while the same iterative error for ODE45 at the same number of iterations is 10^{-1} for the same value of β. We also noted that the times to converges to the solution using SQLM is in general 10 times more quickly than the time to converge using ODE45. For HAM it takes several minutes. We conclude that the SQLM method is more accurate and efficient than the ODE45 method and HAM. On the physical interpretation of the results that depend on the dimensionless pressure gradient parameter β, we found that when β increase the skin friction, the shear stress, the friction coefficient and the drag force also increases. Only the displacement thickness decrease in this case. When β decreases, the skin friction, the shear stress, the friction coefficient and the drag force also decreases. In this case, the displacement thickness increase. For a specific value of $\beta = -0.19884$, all the parameters are zero except the displacement thickness which reaches its largest size. This corresponds to an angle of 18^o.

Keywords: *Boundary layer*, *Falkner-Skan equations*, *HAM*, *SQLM*, *ODE45*.

Declaration

I, the undersigned, hereby declare that the work contained in this research project is my original work, and that any work done by others or by myself previously has been acknowledged and referenced accordingly.

Yannick Harisson NKOCKO AWOUNTSA, 24 October 2019

List of abbreviations

HAM	homotopy analysis method
HPM	homotopy perturbation method
ODE	ordinary differential equation
OHAM	optimal homotopy analysis method
PDE	partial differential equation
QLM	quasi-linearisation method
SQLM	spectral quasi-linearisation method

Contents

1. Introduction

In physics and fluid mechanics, a boundary layer is an important concept and refers to the layer of fluid in the immediate vicinity of a bounding surface where the effects of viscosity are significant (Wikipedia). A boundary layer comes into the picture when a fluid is interacting with a solid surface during its flow. For example, in the Earth's atmosphere, the boundary layer is the layer of air near the ground. On the wings of an airplane, it is the air that develops directly on the surface of the airplane wing and is only a few millimetres thick. This phenomenon has many applications particularly in engineering (automotive and aeronautical) where the boundary layer thickness depends on the velocity of the air and Reynolds number. The equations arising from this boundary layer are not easy to solve. To be able to solve the boundary layer equations, a common procedure is to transform them using suitable similarity variables to obtain the so-called Falkner-Skan equations.

In fluid dynamics, the Falkner-Skan boundary layer, for example, describes the steady two-dimensional laminar boundary layer that forms a wedge in which the plate is not parallel to the flow (VM and SW, 1931). The Falkner-Skan equations are obtained by the reduction of Navier-Stokes equations to boundary layer equations (Prandtl, 1904). These equations are described by a nonlinear ordinary differential equation (ODE). That is a generalization of the Blasius equation (Blasius, 1908). The Falkner-Skan equations are nonlinear equations which makes it difficult to find the exact analytical solution. Approximate solutions have been found using semi-analytical and numerical methods.

1.1 Semi-analytical methods

Of the common semi-analytical methods, we can mention the perturbation method (He, 2003), the optimal homotopy analysis method (OHAM) (Marinca et al., 2014), the homotopy perturbation method (HPM) (Moallemi et al., 2012) and the homotopy analysis method (HAM)(Liao, 1999b), (Barania et al., 2012). All these semi-analytical methods have their own strengths and drawbacks.

The perturbation method requires the presence of a small parameter in the nonlinear equation and the approximate solution of the equation containing this parameter is expressed as series expansions in a small parameter. The selection of a small parameter requires a special skill. Choosing an appropriate small parameter gives acceptable results while an improper choice may result in incorrect solutions. Also, most fluid dynamic equations do not deal with small parameters. For example, the Falkner-Skan equations do not have a small parameter.

Liao (1999b) proposed the so-called homotopy analysis method to solve equations for a two-dimensional viscous flow over a semi-infinite plate. This method is based on the homotopy method in topology and is independent of whether or not nonlinear problems contain small parameters. Therefore, the HAM is valid for more nonlinear problems, especially those with strong nonlinearity. The HAM is more general and includes the homotopy perturbation method. This method provides us with great freedom to select initial guess approximations and auxiliary parameters. It is this freedom which makes it easier to ensure that the corresponding approximation sequence given by HAM is convergent. The only problem with this method is that it is hard to compute the so-called convergence controlling parameter.

Marinca et al. (2014) found the approximate solution of the Falkner-Skan equations using an approximate technique called the optimal homotopy asymptotic method. Much like the homotopy analysis method, this method does not depend on small parameters and provides a convenient way to optimally control the convergence of the approximate solutions. This method is very simple and accurate.

Hartree (1937) showed that the physical solution of Falkner-Skan equations can be interpreted only if β is in the range $-0.19884 \leq \beta \leq 2$ (decelerating flows for $-0.19884 \leq \beta \leq 0$ and accelerating flows for $0 \leq \beta \leq 2$). Knowing that all these methods can not find the exact analytical solution of Falkner-Skan equations, and noticing that some are time-consuming, many researchers prefer to use numerical methods to find the solutions of Falkner-Skan equations.

1.2 Numerical methods

There exist many numerical methods in the literature which may be used to solve the Falkner-Skan equations. We can mention the high order compact finite difference schemes (Duque-Daza et al., 2011), the shooting technique (Parveen, 2014), (Asaithambi, 1997), the spectral collocation method (Parand et al., 2011), the Keller Box method (Ishak et al., 2007), the quasi-linearisation method (QLM) (Zhu et al., 2009) and finite elements. All these numerical methods have their own strengths and drawbacks.

Zhu et al. (2009) used the QLM method to solve the Falkner-Skan equations. This quasi-linearisation method is based on the Newton–Raphson method for solving a nonlinear n^{th} order ordinary or partial differential equation in *N* dimensions as a limit of a sequence of linear differential equations. The QLM goal is to linearize and decouple a nonlinear equation in terms of a finite set of equations which can often be solved analytically or numerically in a convenient fashion using superposition. In addition, the QLM sequence gives quadratic convergence and monotonicity.

Ishak et al. (2007) used the Keller Box method to solve the Falkner-Skan equations. This method works as follow: reduce the Falkner-Skan equations to a first-order system, write this system in difference form using central differences, solve the resulting algebraic equations using Newton's method, writing the linearized equations in matrix-vector using the block-tridiagonal-elimination technique.

The spectral quazi-linearisation method (SQLM) is a new type of method which is an improvement of the QLM. When the Chebyshev spectral method is used to solve the linearized equation, the method is called the spectral quasi-linearisation method. This method converges generally to the solution just after four iterations and the time to converge is very small.

1.3 Aims and objectives

1.3.1 Aims.

The main aim of this project is to compare the semi-analytical and numerical methods for solving Falkner-Skan equations. In so doing, physical quantities such as the skin friction, shear stress, friction coefficient, total friction force, and displacement thickness will be studied.

1.3.2 Objectives.

The objectives of this study are the following

- Derive the Falkner-Skan equations starting from Navier-Stokes equations.
- Analyse Falkner-Skan equations for stagnation point flow, flow past a wedge, flow past a flat plate, flow around a corner and flow due to a line sink.
- Find the semi-analytical solution of the Falkner-Skan equations using the homotopy analysis method.
- Find numerical solution using spectral quasi-linearisation method and ODE45.

• Compare the analytical and numerical solutions

• Compute and explain the following quantities for certain types of fluid flow: skin friction, shear stress, friction coefficient, friction force, and displacement thickness.

1.4 Layout

This thesis is organized as follows: in Chapter 2, we derive the Falkner-Skan equations starting from Navier-Stokes equations and we analyse the equations for different types of fluid flow, in Chapter 3 we present the methods that are used to solve the Falkner-Skan equations. Concerning the semi-analytical and numerical methods the HAM, the SQLM and the MATLAB function ODE45 are used. In Chapter 4 we apply these methods to solve the Falkner-Skan equations. The result and discussion will be analysed in Chapter 5. The conclusion will be part of Chapter 6.

2. Derivation and analysis of the Falkner-Skan equations

To obtain the Falkner-Skan equations, we start with the Navier-Stokes equations, reduce by using certain hypotheses to obtain the boundary layer equations. We reduce the boundary layer equations to an ODE by using similarity analysis.

2.1 Navier-Stokes Equations

Navier-Stokes equations are nonlinear partial differential equations that describe the movement of real fluids such as gases and liquids. The compressible (most general) Navier-Stokes momentum equation is given by

$$\rho\left(\frac{\partial u}{\partial t} + u.\nabla u\right) = -\nabla p + \mu\nabla^2 u + \frac{1}{3}\mu\nabla(\nabla.u) + \rho g, \tag{2.1.1}$$

where ρ, u, g,μ,∇, t and p are respectively the density, flow velocity, body acceleration, dynamic viscosity, the Laplacian, time and pressure. The continuity equation is given by

$$\frac{\partial \rho}{\partial t} + \nabla.(\rho u) = 0. \tag{2.1.2}$$

For the special case of an incompressible flow ($\rho =$ constant), so the continuity equation reduces to

$$\nabla.u = 0, \tag{2.1.3}$$

and Equation (2.1.1) reduces to

$$\rho\left(\frac{\partial u}{\partial t} + u.\nabla u\right) = -\nabla p + \mu\nabla^2 u + \rho g. \tag{2.1.4}$$

The solution to Equation (2.1.4) is very difficult to obtain. To solve Equations (2.1.4) and (2.1.3), researchers make various assumptions in order to reduce the Navier-Stokes equations. The well known reduced Navier-Stokes equations are the boundary layer equations.

2.2 Boundary Layer Equations

The German mathematician Prandtl (Prandtl, 1904) developed the boundary layer theory and derived the boundary layer flow equations by reducing the Navier-Stokes equations.

A boundary layer is an important concept in fluid mechanics and refers to the fluid layer in the immediate vicinity of a boundary surface where viscosity effects are significant.

A boundary layer comes into the picture when a fluid is interacting with a solid surface during its flow. So a boundary layer is a thin layer of fluid over the surface of the body when there is a fluid flow over the body.

2.2.1 Prandtl Hypothesis.

To reduce the Navier-Stokes equations, Prandtl made the following assumptions (nptel)

1-For fluids with low viscosity, the effect of internal friction in the fluid are significant only in a narrow region around the boundaries of the solid on which the fluid flows.

2-Near the body is located the boundary layer where shear stresses exert a more and more important effect on the fluid as one moves from the free surface to the surface of the solid.

3-Outside the boundary layer, the effect of shear stresses on the flow is small compared to the values inside the boundary layer. Therefore, with the exception of the immediate vicinity of the surface, the flow is frictionless and the velocity is the free stream velocity.

4-The transition from the main velocity from zero to the surface takes place through the boundary layer.

2.2.2 Boundary Conditions.

1-On the surface of the solid boundary the fluid is stationary (see Figure 2.1), hence

$$u = 0, \tag{2.2.1}$$

where u is the free stream component of the velocity.

2-On the free stream

$$u = U, \tag{2.2.2}$$

where U is the free stream velocity.

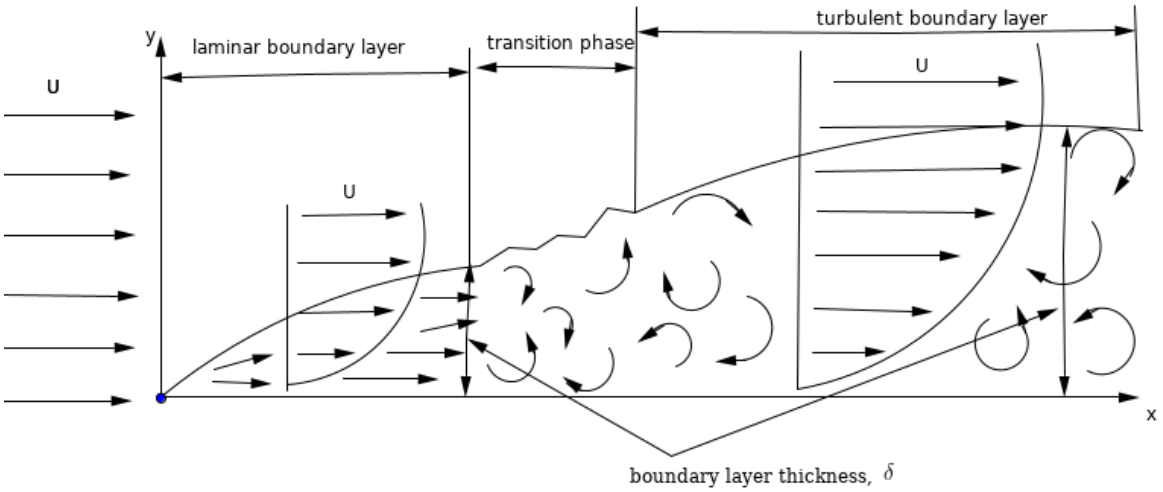

Figure 2.1: Boundary layer

2.2.3 Boundary layer approximation.

1-The velocity at the outer edge of the boundary layer is of the order U.

2-The derivatives in the x-direction can be estimated by means of a characteristic length L.

3-The thickness of the boundary layer has a characteristic size δ with $\delta << L$. The derivatives in y-direction also have a characteristic size δ.

4-No external influence exists.

Let us consider the Navier-Stokes equations for steady ($\frac{\partial}{\partial t} = 0$), two dimensional (2D), incompressible flow ($\nabla.u = 0$), cartesian coordinate system (x,y), velocity component (u,v). The equations of motion for steady two-dimensional incompressible flow are

$$\frac{\partial u}{\partial x} + \frac{\partial v}{\partial y} = 0, \qquad \text{continuity equation} \tag{2.2.3}$$

$$u\frac{\partial u}{\partial x} + v\frac{\partial u}{\partial y} = -\frac{1}{\rho}\frac{\partial p}{\partial x} + \nu\left(\frac{\partial^2 u}{\partial x^2} + \frac{\partial^2 u}{\partial y^2}\right), \qquad \text{x-momentum equation} \tag{2.2.4}$$

$$u\frac{\partial v}{\partial x} + v\frac{\partial v}{\partial y} = -\frac{1}{\rho}\frac{\partial p}{\partial y} + \nu\left(\frac{\partial^2 v}{\partial x^2} + \frac{\partial^2 v}{\partial y^2}\right). \qquad \text{y-momentum equation} \tag{2.2.5}$$

Our goal is to reduce Equations (2.2.3), (2.2.4) and (2.2.5) using scaling analysis.

Applying scaling analysis to continuity Equation (2.2.3), we find that

$\frac{\partial u}{\partial x} \sim \frac{U}{L}$ (a) and $v \sim \frac{\delta U}{L}$ (b).

Doing the same to x-momentum and y-momentum Equations (2.2.4),(2.2.5) we find also that

$u\frac{\partial u}{\partial x} \sim \frac{U^2}{L}$ (c), $v\frac{\partial\, u}{\partial y} \sim \frac{U^2}{L}$ (d), $\frac{\partial^2 u}{\partial y^2} \sim \frac{U}{\delta^2}$ (e), $\frac{\partial^2 u}{\partial x^2} \sim \frac{U}{L^2}$ (f), $\frac{1}{\rho}\frac{\partial p}{\partial x} \sim \frac{U^2}{L}$ (g)

$u\frac{\partial v}{\partial x} \sim \frac{\delta U^2}{L^2}$ (h), $v\frac{\partial v}{\partial y} \sim \frac{\delta U^2}{L^2}$ (i), $\frac{\partial^2 v}{\partial x^2} \sim \frac{\delta U}{L^3}$ (j), $\frac{\partial^2 v}{\partial y^2} \sim \frac{U}{\delta L}$ (k) and $\frac{1}{\rho}\frac{\partial p}{\partial y} \sim \frac{U^2\delta}{L^2}$ (l)

Now let us use them to reduce the Navier-Stokes equations.

• Let us compare (f) and (e)

$$\frac{(e)}{(f)} = \frac{\frac{U}{\delta^2}}{\frac{U}{L^2}} = \frac{L^2}{\delta^2} = \left(\frac{L}{\delta}\right)^2.$$

Since $\frac{L}{\delta} >> 1 \Rightarrow (e) >> (f)$. Then $\frac{\partial^2 u}{\partial y^2} >> \frac{\partial^2 u}{\partial x^2}$ and we can neglect $\frac{\partial^2 u}{\partial x^2}$ behind $\frac{\partial^2 u}{\partial y^2}$.

We can rewrite Equation (2.2.4) as

$$u\frac{\partial u}{\partial x} + v\frac{\partial u}{\partial y} = -\frac{1}{\rho}\frac{\partial p}{\partial x} + \nu\frac{\partial^2 u}{\partial y^2}. \tag{2.2.6}$$

• Dividing (l) and (g), we have

$$\frac{(l)}{(g)} = \frac{\frac{U^2\delta}{L^2}}{\frac{U^2}{L}} = \frac{\delta}{L} \Rightarrow \frac{\partial p}{\partial y} << \frac{\partial p}{\partial x}.$$

So we can conclude that $\frac{\partial p}{\partial y} = 0$ and write

$$\frac{1}{\rho}\frac{\partial p}{\partial y} = 0. \tag{2.2.7}$$

Finally the continuity equation and Navier-Stokes equations reduce to

$$\frac{\partial u}{\partial x} + \frac{\partial v}{\partial y} = 0, \tag{2.2.3}$$

$$u\frac{\partial u}{\partial x} + v\frac{\partial u}{\partial y} = -\frac{1}{\rho}\frac{\partial p}{\partial x} + \nu\frac{\partial^2 u}{\partial y^2}, \tag{2.2.7}$$

$$\frac{1}{\rho}\frac{\partial p}{\partial y} = 0. \tag{2.2.8}$$

These equations are called boundary layer equations or Prandtl equations and the corresponding boundary conditions are

$$y = 0, \quad u = v = 0 \qquad (2.2.8) \qquad \text{and} \qquad y = \infty, \quad u = U(x). \qquad (2.2.9)$$

An interesting aspect of the boundary layer equations is that they can help us to express inside boundary layer the following terms: velocity field, boundary layer thickness, shear stress distribution and drag force on the plate. To solve, we need to transform the equations into an ordinary differential equation (ODE). The most known equations which have been obtained by using Prandtl equations are Blasius equations and Falkner-Skan equations. The Falkner-Skan equations is a generalisation of Blasius equations.

The equations which interests us here are Falkner-Skan equations. In the next paragraph, we will show how to obtain Falkner-Skan equations starting from boundary layer equations.

2.3 Falkner-Skan Equations

2.3.1 Falkner-Skan hypothesis.

- We consider a two-dimensional laminar boundary layer, steady, incompressible Navier-Stokes equations.
- Consider flows where the plates are not parallel to the fluid flow.
- The external velocity is $U(x) \neq 0$.
- Similarity analysis is performed.

2.3.2 Starting point.

We start from the Prandtl Equations (2.2.3),(2.2.7),(2.2.8)

$$\frac{\partial u}{\partial x} + \frac{\partial v}{\partial y} = 0, \tag{2.2.3}$$

$$u\frac{\partial u}{\partial x} + v\frac{\partial u}{\partial y} = -\frac{1}{\rho}\frac{\partial p}{\partial x} + \nu\frac{\partial^2 u}{\partial y^2}, \tag{2.2.7}$$

$$\frac{1}{\rho}\frac{\partial p}{\partial y} = 0. \tag{2.2.8}$$

subject to the boundary conditions

$$y = 0, \quad u = v = 0 \qquad (2.2.9) \qquad \text{and} \qquad y = \infty, \quad u = U(x). \qquad (2.2.10)$$

Using Equation (2.2.8), we see that

$$\frac{\partial p}{\partial y} = 0 \Rightarrow p = p(x).$$

Since $p = p(x)$, we can now applied Bernoulli's equation in order to find the pressure. We have

$$p + \frac{1}{2}\rho U^2(x) = Cte \Rightarrow -\frac{1}{\rho}\frac{dp}{dx} = U\frac{dU}{dx}. \qquad (2.3.1)$$

Substituting (2.3.1) into (2.2.7), we have

$$u\frac{\partial u}{\partial x} + v\frac{\partial u}{\partial y} = U\frac{dU}{dx} + \nu\frac{\partial^2 u}{\partial y^2}. \qquad (2.3.2)$$

To be able to transform (2.2.3) and (2.3.2) into an ODE similarity analysis is used. In order to perform a similarity analysis in Equation (2.2.3), Falkner and Skan propose the following transformation

$$\xi(x, y) = y\sqrt{\frac{U}{\nu x}}, \qquad (2.3.3)$$

and an implicit dimensionless stream function $g[\xi(x, y)]$ such that

$$\Psi(x, \xi) = \sqrt{U\nu x}\, g[\xi(x, y)], \qquad (2.3.4)$$

where Ψ is a conventional stream function. The relation between velocity and stream function are given by

$$u = \frac{\partial \Psi}{\partial y}, \qquad (2.3.5)$$

$$v = -\frac{\partial \Psi}{\partial x}. \qquad (2.3.6)$$

Substituting $\Psi(x, \xi)$ and $\xi(x, y)$ by their expression (2.3.3) and (2.3.4) we find

$$u = Ug', \qquad (2.3.7)$$

$$v = \frac{1}{2}\sqrt{\frac{\nu U}{x}}\left[\xi g' - g\right] - \frac{1}{2}\sqrt{\frac{\nu x}{U}}\frac{dU}{dx}g, \qquad (2.3.8)$$

$$\frac{\partial u}{\partial y} = U\sqrt{\frac{U}{\nu x}}g'', \qquad (2.3.9)$$

$$\frac{\partial^2 u}{\partial y^2} = \frac{U^2}{\nu x}g''', \qquad (2.3.10)$$

$$\frac{\partial u}{\partial x} = g'\frac{dU}{dx} - \frac{1}{2}\frac{U}{x}\xi g''. \qquad (2.3.11)$$

Substituting (2.3.11),(2.3.10),(2.3.9),(2.3.8) and (2.3.7) into (2.3.2) and after developing we obtain

$$U\frac{dU}{dx}g'^2 - \frac{1}{2}\frac{U^2}{x}gg'' - \frac{1}{2}U\frac{dU}{dx}gg'' = U\frac{dU}{dx} + \frac{U^2}{x}g''',$$

and dividing by $\frac{U^2}{x}$ we obtain

$$g''' + \frac{1}{2}\left[1 + \frac{x}{U}\frac{dU}{dx}\right]gg'' + \frac{x}{U}\frac{dU}{dx}\left[1 - g'^2\right] = 0.$$

Setting $\gamma = \frac{x}{U}\frac{dU}{dx}$ the dimensionless pressure gradient parameters, our previous expression becomes

$$\frac{d^3g}{d\xi^3} + \frac{\gamma+1}{2}g\frac{d^2g}{d\xi^2} + \gamma\left[1 - \left(\frac{dg}{d\xi}\right)^2\right] = 0. \tag{2.3.12}$$

Equation (2.3.12) is called Falkner Skan equations with the boundary conditions

$$\xi = 0, \quad g = g' = 0 \tag{2.3.13}$$

and

$$\xi \mapsto \infty, \quad g' = 1. \tag{2.3.14}$$

Hartree (1937) introduced additional simplification to Equation (2.3.12) by defining the following linear transformation

$$\eta = \sqrt{\frac{\gamma+1}{2}}\xi, \text{ and } f = \sqrt{\frac{\gamma+1}{2}}g. \tag{2.3.15}$$

After deriving and substitute into Equation (2.3.12), we find

$$\frac{d^3f}{d\eta^3} + f\frac{d^2f}{d\eta^2} + \beta\left[1 - \left(\frac{df}{d\eta}\right)^2\right] = 0, \tag{2.3.16}$$

where $\beta = \frac{2\gamma}{\gamma+1}$ is a dimensionless pressure gradient parameter. It is also noted that when $\beta = 0$, we obtain the Blasius equation. When $\beta > 0$, we are working with a favourable pressure gradient $(\frac{\partial p}{\partial x} < 0)$. When $\beta < 0$, we have an adverse pressure gradient $(\frac{\partial p}{\partial x} > 0)$. Equation (2.3.16) is the most known form of Falkner Skan equations and the new boundary conditions are

$$\eta = 0, \quad f = f' = 0 \tag{2.3.17}$$

and

$$\eta \mapsto \infty, \quad f' = 1. \tag{2.3.18}$$

2.4 Analysis of Falkner-Skan Equations

In the Falkner-Skan equations, the parameter β is an important parameter because it allows us to differentiate different types of fluid flow. In this section, we analyse the Falkner-Skan equations for stagnation point flow, flow past a wedge, flow past a flat plate, flow around a corner and flow due to a line sink.

2.4.1 Stagnation point flow.

For a stagnation point flow, the plate is perpendicular to the fluid flow. The fluid hits the plate before changing direction. The fluid which was perhaps horizontal at the beginning becomes vertical after hitting the plate (see Figure 2.1a). In this case $\beta = 1$, therefore $\gamma = 1$ and the Falkner-Skan equations becomes

$$\frac{d^3f}{d\eta^3} + f\frac{d^2f}{d\eta^2} + \left[1 - \left(\frac{df}{d\eta}\right)^2\right] = 0. \tag{2.4.1}$$

2.4.2 Flow past a flat plate.

Here the plate is flat and the fluid flow is parallel to the plate (see Figure 2.1b). In a flow past a flat plate $\beta = 0$, so that $\gamma = 0$ and the Falkner-Skan equations becomes

$$\frac{d^3f}{d\eta^3} + f\frac{d^2f}{d\eta^2} = 0. \tag{2.4.2}$$

Equation (2.4.2) is the Blasius equation.

2.4.3 Flow past a wedge.

Here, the plate makes a certain angle α $(0 \leqslant \alpha \leqslant \frac{\pi}{2})$ with the horizontal (see Figure 2.1c) and the fluid which at the beginning was horizontal is deviated by the same angle.

Consider the flow $(0 < \theta < 2\pi - \pi\beta_1)$ past a wedge of angle $\frac{\pi}{2}\beta_1 = \alpha$. Then α can take only the value between 0 and $\frac{\pi}{2}$ i.e. $\alpha \in [0, \frac{\pi}{2}]$. This condition is satisfied if and only if $0 \leqslant \beta_1 \leqslant 1$ and multiplying by 2 we have $0 \leqslant \beta \leqslant 2$. Since $\beta = \dfrac{2\gamma}{\gamma+1}$ then we have $0 \leqslant \gamma \leqslant \infty$. The Falkner-Skan equations becomes

$$\frac{d^3f}{d\eta^3} + f\frac{d^2f}{d\eta^2} + \beta\left[1 - \left(\frac{df}{d\eta}\right)^2\right] = 0, \quad \text{with} \quad 0 \leqslant \beta \leqslant 2. \tag{2.4.3}$$

2.4.4 Flow around a corner.

Here, the plate makes an angle α with the horizontal and the fluid which at the beginning was horizontal is deviated of the same angle (see Figure 2.1d). Consider a flow around a corner of angle $\frac{\pi}{2}\beta_1 = \alpha$. The minimum value of α is $\alpha_{min} = -\frac{\pi}{2}$ and maximum value of α is $\alpha_{max} = 0$. Then, $\alpha \in [-\frac{\pi}{2}, 0]$ and this condition is satisfied if $-1 \leqslant \beta_1 \leqslant 0$ and multiplying by 2 we have $-2 \leqslant \beta \leqslant 0$. Since $\beta = \dfrac{2\gamma}{\gamma+1}$ then we have $-\frac{1}{2} \leqslant \gamma \leqslant 0$. The Falkner-Skan equations is rewritten as

$$\frac{d^3f}{d\eta^3} + f\frac{d^2f}{d\eta^2} + \beta\left[1 - \left(\frac{df}{d\eta}\right)^2\right] = 0, \quad \text{with} \quad -2 \leqslant \beta \leqslant 0. \tag{2.4.4}$$

2.4.5 Flow due to a line sink.

In this case, $\gamma = -1$ and $\beta = \infty$ (see Figure 2.1e) and the Falkner-Skan equations reduces in the limit to

$$1 - f'^2 = 0 \Rightarrow f'' = 0, \quad \text{at} \quad \eta \mapsto \infty. \tag{2.4.5}$$

Since $\gamma = -1$, using (2.3.15), we have

$$\eta = 0, \ \text{ and } \ f = 0, \tag{2.4.6}$$

which is absurd. So we have to introduce the new additional simplification. Our goal is to find a way to write a new linear transformation which is independent of γ. Before that, let us find the relation between the velocity of U and the direction x. For flow due to a line sink, the velocity U and x direction have to be in the opposite direction. Using the dimensionless pressure gradient, i.e. $\gamma = \frac{x}{U}\frac{dU}{dx}$ we have

$$\gamma = -1 \Rightarrow \frac{c}{x} = U. \tag{2.4.7}$$

So for a flow due to a line sink, the velocity is given by $U = \frac{c}{x}$ where c is a constant. Equation (2.3.15) is defined as

$$\eta = \sqrt{\frac{\gamma+1}{2}}\xi = \sqrt{\frac{(\gamma+1)U}{2\nu x}}y. \tag{2.4.8}$$

Since $\gamma = -1$, according to (2.4.8) we easily see that $\eta = 0$. Our goal is to find a way to write a new linear transformation which is independent of γ. For doing that we introduce a new variable

$$Y = \sqrt{-\frac{2}{\gamma+1}}\eta = \sqrt{-\frac{U}{\nu x}}y. \tag{2.4.9}$$

We use the sign "-" because U and x are in the opposite direction. Doing the same to the second Equation (2.3.15) $f = \sqrt{\frac{\gamma+1}{2}}g$, we introduce the new variable

$$F = \sqrt{-\frac{2}{\gamma+1}}f, \tag{2.4.10}$$

and rewriting the Falkner-Skan equations in terms of the new variable F and Y we obtain

$$\frac{d^3F}{dY^3} - \frac{\gamma+1}{2}F\frac{d^2F}{dY^2} - \gamma\left[1 - \left(\frac{dF}{dY}\right)^2\right] = 0.$$

Setting $\gamma = -1$, the previous equation reduces to

$$\frac{d^3F}{dY^3} - \left(\frac{dF}{dY}\right)^2 + 1 = 0. \tag{2.4.11}$$

- The corresponding boundary condition are

$$Y = 0, \quad F = F' = 0 \tag{2.4.12}$$

$$Y \mapsto \infty, \ F' = 1 \text{ and } F'' = 0. \tag{2.4.13}$$

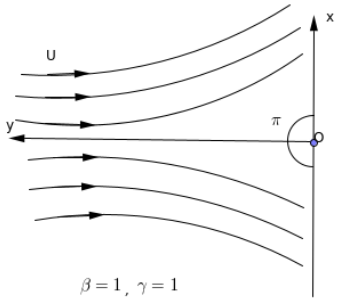

(a) Stagnation point flow

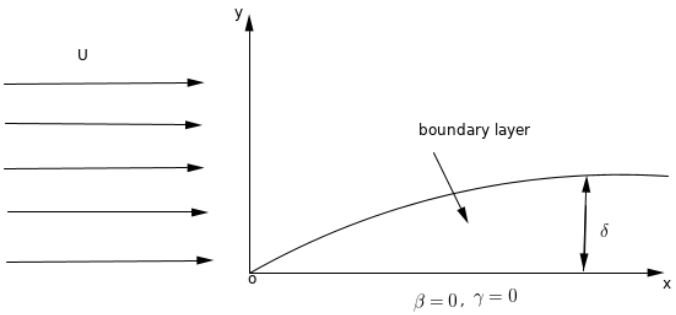

(b) Flow past a flat plate

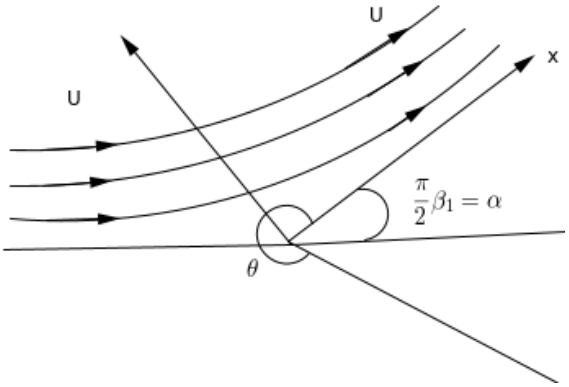

(c) Flow past a wedge

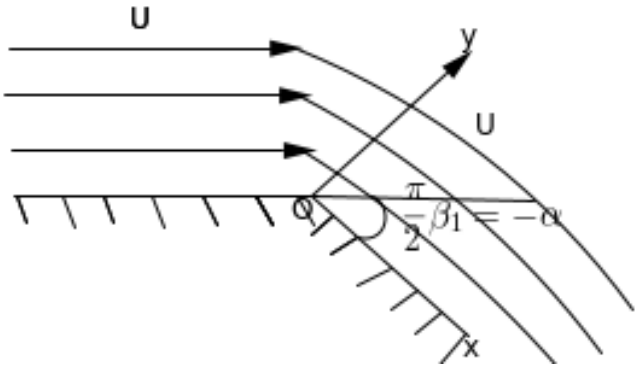

(d) Flow around a corner

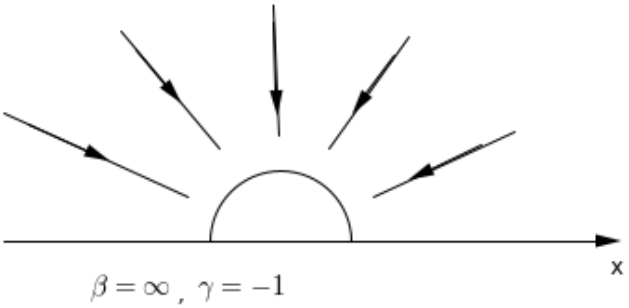

(e) Flow due to a line sink

Figure 2.2: Different types of fluid flow

3. Methods of solution

In this chapter, we present the semi-analytical and numerical methods that we use to solve the Falkner-Skan equations. We use homotopy analysis method (HAM) for semi-analytical method, the spectral qazi-linearisation method (SQLM) and MATLAB function ODE45 for the numerical methods.

3.1 Homotopy Analysis Method

The homotopy analysis method is a semi-analytical method whose main objective is to solve nonlinear differential equations. The homotopy analysis method is based on homotopy in topology and generates convergent series solutions for nonlinear equations. This is possible by using a homotopy-Maclaurin series to handle the nonlinearities of the system.

The HAM was first described by Liao in his doctoral dissertation (Liao, 1992). Later, it was modified to introduce a nonzero auxiliary parameter (Liao, 1999a). This parameter serves to ensure convergence and is labelled $\hbar$.

3.1.1 Brief description of the method.

For solving nonlinear ODEs or nonlinear PDEs, we can follow these steps.

•Step 1: Consider these general nonlinear differential equations

$$\mathcal{N}[u(x)] = 0, \tag{3.1.1}$$

where $\mathcal{N}$ ia a nonlinear operator and x the independent variable of the function.

•Step 2: We construct the zeroth-order deformation equation

$$(1-p)\mathcal{L}[U(x,p) - u_0(x)] = \hbar p \mathcal{N}[U(x,p)], \tag{3.1.2}$$

where $p \in [0,1]$ is the embedded parameter, $\mathcal{L}$ the auxiliary linear operator, $\hbar$ an auxiliary parameter (called the convergence-control parameter), $U(x,p)$ the unknown function, $u_0(x)$ our initial guess.

Always remember that when $p = 0$, we have $U(x,0) = u_0(x)$ and when $p = 1$ we have $U(x,1) = u(x)$. We said that the solution varies from the initial guess $u_0(x)$ to the solution $u(x)$.

•Step 3: We use the Taylor series expansions to expend $U(x,p)$ and we obtain this general expression

$$U(x,p) = u_0(x) + \sum_{m=1}^{\infty} u_m(x) p^m, \tag{3.1.3}$$

where

$$u_m(x) = \frac{1}{m!} \frac{\partial^m U(x,p)}{\partial p^m}|_{p=0}. \tag{3.1.4}$$

When $p = 1$, we have

$$u(x) = u_0(x) + \sum_{m=1}^{\infty} u_m(x). \tag{3.1.5}$$

•Step 4: We differentiate the zeroth-order deformation equation (3.1.2) m-times with respect to p and then dividing by $m!$ and setting $p = 0$, we get the following m-order deformation equation

$$\mathcal{L}[u_m(x) - \chi_m u_{m-1}(x)] = \hbar R_m[u_0, u_1, ..., u_{m-1}]; \tag{3.1.6}$$

where

$$R_m[u_0, u_1, ..., u_{m-1}] = \frac{1}{m!}\frac{\partial^m N[U(x,p)]}{\partial p^m}|_{p=0}. \tag{3.1.7}$$

Notice that $\chi_1 = 0$, $\chi_k = 1$ for $k > 1$, R_m depend only on $u_0, u_1, ..., u_{m-1}$ and can be computed easily using Mathematica or Maple software. In this way, the original nonlinear equation is transferred into an infinite number of linear ones, but without the assumption of any small/large physical parameters.

3.2 Spectral Quasi-Linearisation Method

3.2.1 Chebyshev spectral differentiation matrices.

In this section, we discuss the development of the spectral differentiation matrices. Suppose we want to approximate the derivative of the function $q(x)$ with respect to x. Firstly we approximate the function using a grid points

$$x_0, x_1, x_2, ..., x_{N-1}, x_N,$$

where x_j for $j = 0, 1, 2, 3, ..., N$ is defined as

$$x_j = cos\frac{\pi j}{N}, \qquad j = 0, 1, 2, 3, ..., N. \tag{3.2.1}$$

The grid points defined using (3.2.1) are called Chebyshev-Gauss-Lobatto nodes. Let us assume that the value of $q(x)$ at the grid points is given by $q_m = q(x_m)$. Using the Lagrange interpolation polynomials, we approximate the function $q(x)$ as

$$q(x) \approx Q_N(x) = \sum_{m=0}^{N} q_m L_m(x), \tag{3.2.2}$$

where we define L_m as the Lagrange interpolation polynomials,

$$Ł_m(x_j) = \begin{cases} 1, & if \quad j = m; \\ 0, & if \quad j \neq m. \end{cases} \tag{3.2.3}$$

In order to approximate $q'(x)$, we differentiate equation (3.2.2) and we obtain

$$q'(x) = \sum_{m=0}^{N} q_m L'_m(x). \tag{3.2.4}$$

The collocation process involves evaluating functions at chosen grid points and their derivatives. Evaluating (3.2.4) at the grid points $\{x_j\}$ give us

$$q'(x_j) = \sum_{m=0}^{N} q_m L'_m(x_j) = \sum_{m=0}^{N} P_{jm} q_m, \qquad j = 0, 1, 2, 3, ..., N, \tag{3.2.5}$$

where

$$P_{jm} = L'_m(x_j).$$

In vector form, it is possible to express equation (3.2.5) in the following form

$$\begin{pmatrix} P_{0,0} & P_{0,1} & P_{0,2} & . & . & . & P_{0,N-1} & P_{0,N} \\ P_{1,0} & P_{1,1} & P_{1,2} & . & . & . & P_{1,N-1} & P_{1,N} \\ P_{2,0} & P_{2,1} & P_{2,1} & . & . & . & P_{2,N-1} & P_{2,N} \\ . & . & . & . & . & . & . & . \\ . & . & . & . & . & . & . & . \\ . & . & . & . & . & . & . & . \\ P_{N-1,0} & P_{N-1,1} & P_{N-1,1} & . & . & . & P_{N-2,N-1} & P_{N-2,N} \\ P_{N,0} & P_{N,1} & P_{N,2} & . & . & . & P_{N,N-1} & P_{N,N} \end{pmatrix} \begin{pmatrix} q(x_0) \\ q(x_1) \\ q(x_2) \\ . \\ . \\ . \\ q(x_{N-1}) \\ q(x_N) \end{pmatrix} = \begin{pmatrix} q'(x_0) \\ q'(x_1) \\ q'(x_2) \\ . \\ . \\ . \\ q'(x_{N-1}) \\ q'(x_N) \end{pmatrix}. \tag{3.2.6}$$

The above matrix equation can be written compactly as

$$\mathbf{Q'} \approx P\mathbf{Q}, \tag{3.2.7}$$

where **Q** and **Q'** are given by $\mathbf{Q'} = [q'(x_0), q'(x_1), ..., q'(x_N)]^T$, $\mathbf{Q} = [q(x_0), q(x_1), ..., q(x_N)]^T$. The entries of the matrix P are P_{jm} with $j, m = 0, 1, 2, 3, ..., N$.

The higher order derivatives are defined as follows

$$\mathbf{Q''} \approx P^2\mathbf{Q}, \quad \mathbf{Q'''} \approx P^3\mathbf{Q}, \quad \text{etc.} \tag{3.2.8}$$

3.2.2 Solving nonlinear boundary value problems using quasi-linearisation method.

In this section, we present the quasi-linearisation method approach to simplify nonlinear ordinary differential equations. The method is called the spectral quasi-linearization method when the spectral method is used to solve the linearized equation. The following nonlinear ordinary differential equation is considered to demonstrate the development of the QLM iteration scheme

$$Q[x, y(x), y'(x), ..., y^l(x)] = 0, \qquad x \in [c, d], \tag{3.2.9}$$

with the limits

$$J_{c,m}[y(c), y'(c), ..., y^n(c)] = 0, \qquad m = 1, 2, 3, ...k \tag{3.2.10}$$

$$J_{d,m}[y(d), y'(d), ..., y^l(d)] = 0, \qquad m = k+1, k+2, k+3...l, \tag{3.2.11}$$

where Q is a nonlinear $y(x)$ operator and its l derivatives, $J_{c,n}$, $J_{d,n}$ are nonlinear $y(x)$ functions with $x = c$ and $x = d$ for $n = 1, 2, ..., l-1$derivatives.The QLM method assumes that the difference between the current iteration level approximation of the solution (referred to as $y_{i+1}(x)$) and the previous iteration (referred to as $y_i(x)$) is small. Often believed to be minimal is the difference between the derivatives at the following iteration points, $y_{i+1}^{(s)} - y_i^{(s)}$. The QLM defines the approximate solution at the iteration of $(i+1)$ as the linear equation solution

$$Q[x, y_i(x), y_i'(x), ..., y_i^l(x)] + \sum_{s=0}^{l} \frac{\partial Q}{\partial y^{(s)}}[x, y_i(x), y_i'(x), ..., y_i^l(x)]\left(y_{i+1}^{(s)}(x) - y_i^{(s)}(x)\right) = 0, \tag{3.2.12}$$

with linearised limits

$$J_{c,m}[y_i(c), y_i'(c), ..., y_i^l(c)] + \sum_{s=0}^{l-1} \frac{\partial J_{c,m}}{\partial y^{(s)}}[y_i(c), y_i'(c), ..., y_i^l(c)]\left(y_{i+1}^{(s)}(c) - y_i^{(s)}(c)\right) = 0, \tag{3.2.13}$$

for $m = 1, 2, 3, ..., k$ and

$$J_{b,m}[y_i(d), y_i'(d), ..., y_i^l(d)] + \sum_{s=0}^{l-1} \frac{\partial J_{d,m}}{\partial y^{(s)}}[y_i(d), y_i'(d), ..., y_i^l(d)]\left(y_{i+1}^{(s)}(d) - y_i^{(s)}(d)\right) = 0, \tag{3.2.14}$$

for $m = k+1, k+2, k+3..., l$. Since the spectral collocation method of Chebyshev is used to solve nonlinear Equations (3.2.12)-(3.2.14), it is easy to write the equations in the form

$$a_{0,i}(x)y_{i+1}^l(x) + a_{1,i}(x)y_{i+1}^{l-1}(x) + ... + a_{l-1,i}(x)y_{i+1}'(x) + a_{l,i}(x)y_{i+1}(x) = M_i(x), \tag{3.2.15}$$

$$\alpha_{0,m}y_{i+1}^{l-1}(c) + \alpha_{1,m}y_{i+1}^{l-2}(c) + ... + \alpha_{l-2,m}y_{i+1}'(c) + \alpha_{l-1,k}y_{i+1}(c) = M_{c,m}, \tag{3.2.16}$$

$$\beta_{0,m}y_{i+1}^{l-1}(d) + \beta_{1,m}y_{i+1}^{l-2}(d) + ... + \beta_{l-2,m}y_{i+1}'(d) + \beta_{l-1,k}y_{i+1}(d) = M_{d,m}, \tag{3.2.17}$$

where

$$a_{s,i}(x) = \frac{\partial Q}{\partial y^{(l-s)}}[x, y_i(x), y_i'(x), ..., y_i^l(x)], \quad s = 0, 1, 2, 3, .., l, \tag{3.2.18}$$

$$M_i(x) = \sum_{s=0}^{l} \frac{\partial Q}{\partial y^{(s)}}[x, y_i(x), y_i'(x), ..., y_i^l(x)]y_i^s(x) - Q[x, y_i(x), y_i'(x), ..., y_i^l(x)], \tag{3.2.19}$$

$$\alpha_{s,m} = \frac{\partial J_{c,m}}{\partial y^{(s)}}[y_i(c), y_i'(c), ..., y_i^l(c)], \qquad s = 0, 1, 2, 3..., l-1 \quad m = 1, 2, 3..., k. \tag{3.2.20}$$

$$\beta_{s,m} = \frac{\partial J_{d,m}}{\partial y^{(s)}}[y_i(d), y_i'(d), ..., y_i^l(d)], \qquad s = 0, 1, 2, 3..., l-1 \quad m = k+1, k+2, k+3..., l. \tag{3.2.21}$$

$$M_{c,m}(x) = \sum_{s=0}^{l-1} \frac{\partial J_{c,m}}{\partial y^{(s)}}[y_i(c), y_i'(c), ..., y_i^l(c)]y_i^s(c) - J_{c,m}[y_i(c), y_i'(c), ..., y_i^l(c)], \tag{3.2.22}$$

for $m = 1, 2, 3, ..., k$,

$$M_{d,m}(x) = \sum_{s=0}^{l-1} \frac{\partial J_{d,m}}{\partial y^{(s)}}[y_i(d), y_i'(d), ..., y_i^l(d)]y_i^s(d) - J_{d,m}[y_i(d), y_i'(d), ..., y_i^l(d)], \tag{3.2.23}$$

for $m = k+1, k+2, k+3, ..., l$.

The linear QLM iteration schemes (3.2.15) - (3.2.17) is then solved using the Chebyshev spectral collocation method as described in the previous section.

3.3 MATLAB function ODE45

MATLAB's standard solver for ordinary differential equations is the function ODE45. This function implements a Runge-Kutta method with a variable time step for efficient computation. ODE45 is designed to handle the following general problem:

$$\frac{dx}{dt} = g(t, x), \qquad x(t_0) = x_0, \tag{3.3.1}$$

where t and x are respectively the independent variable and dependent variables. $g(t, x)$ is a function of t and x. The mathematical problem is well posed when the functions on the right-hand side of (3.3.1), $g(t, x)$, is pose and initial conditions as, $x = x_0$ and time t_0 are given.

4. Solutions of Falkner-Skan equations

4.1 Analytical and semi-analytical solutions

In this section, we focus on finding exact and semi-analytic solutions for the following cases of fluid flow: stagnation point flow, flow past a wedge, flow past a flat plate, flow around a corner and flow due to a line sink.

4.1.1 Semi-analytical solution of Falkner-Skan equations for $0 \leq \beta \leq 2$.

The Falkner-Skan equations for $0 \leq \beta \leq 2$ is a generalisation of Falkner-Skan equations for the following types of flow: stagnation point flow, flow past a wedge and flow past a flat plate.

Let us consider the Falkner-Skan equations define by Equation (2.3.16)

$$\frac{d^3f}{d\eta^3} + f\frac{d^2f}{d\eta^2} + \beta\left[1 - \left(\frac{df}{d\eta}\right)^2\right] = 0, \quad \eta \in [0, +\infty) \tag{2.3.16}$$

subject to the boundary conditions

$$\eta = 0, \quad f = f' = 0 \tag{2.3.17}$$

and

$$\eta \mapsto \infty, \quad f' = 1. \tag{2.3.18}$$

To solve the Equation (2.3.16) subject to the boundary conditions (2.3.17) and (2.3.18), we use the homotopy analysis method. This method is used in general and does not depend on whether or not nonlinear problems under consideration contain a small parameter.

- Let us consider the following auxiliary linear operator

$$\mathcal{L} = \left(\frac{\partial}{\partial\eta} + \gamma\right)\frac{\partial^2}{\partial\eta^2} = \frac{\partial^3}{\partial\eta^3} + \gamma\frac{\partial^2}{\partial\eta^2}, \tag{4.1.1}$$

where γ is an integer.

- We consider the following guess approximation

$$f_0(\eta) = \eta - \frac{\left[1 - e^{-\gamma\eta}\right]}{\gamma} + \omega\frac{\left[1 - (1+\gamma\eta)e^{-\gamma\eta}\right]}{\gamma^2}, \tag{4.1.2}$$

which satisfies the boundary conditions (2.3.17) and (2.3.18).

- We consider a nonlinear operator

$$N[F(\eta,p)] = \frac{\partial^3 F(\eta,p)}{\partial\eta^3} + F(\eta,p)\frac{\partial^2 F(\eta,p)}{\partial\eta^2} + \beta\left[1 - \left(\frac{\partial F(\eta,p)}{\partial\eta}\right)^2\right]. \tag{4.1.3}$$

We construct the so-called zero-order deformation equation

$$(1-p)\mathcal{L}\Big[F(\eta,p)-f_0(\eta)\Big] = p\hbar N[F(\eta,p)] = p\hbar\Big[\frac{\partial^3 F(\eta,p)}{\partial\eta^3}+F(\eta,p)\frac{\partial^2 F(\eta,p)}{\partial\eta^2}+\beta\Big[1-\Big(\frac{\partial F(\eta,p)}{\partial\eta}\Big)^2\Big]\Big], \tag{4.1.4}$$

where $\eta \in [0,+\infty)$, $\hbar \neq 0$ (auxiliary parameter), $p \in [0,1]$ is the embelding parameter. The boundary condition becomes

$$F(0,p) = F'(0,p) = 0 \quad \text{and} \quad F'(\infty,p) = 1. \tag{4.1.5}$$

• Clearly at $p = 0$, using (4.1.4), we have

$$\mathcal{L}\Big[F(\eta,0) - f_0(\eta)\Big] = 0 \Rightarrow F(\eta,0) = f_0(\eta). \tag{4.1.6}$$

• When p=1, Equation (4.1.4) becomes

$$N[F(\eta,p)] = 0 \Rightarrow \frac{\partial^3 F(\eta,1)}{\partial\eta^3} + F(\eta,1)\frac{\partial^2 F(\eta,1)}{\partial\eta^2} + \beta\Big[1 - \Big(\frac{\partial F(\eta,1)}{\partial\eta}\Big)^2\Big] = 0, \tag{4.1.7}$$

and the boundary condition (4.1.5)

$$F(0,1) = F'(0,1) = 0 \quad \text{and} \quad F'(\infty,1) = 1. \tag{4.1.8}$$

So, when $p = 1$, Equation (4.1.7) and (4.1.8) are the same as (2.3.16), (2.3.17) and (2.3.18) respectively so that we have

$$F(\eta,1) = f(\eta), \quad \eta \in [0,+\infty). \tag{4.1.9}$$

Thus as p increases from 0 to 1, the solution $F(\eta,p)$ varies from the initial $f_0(\eta)$ to the solution $f(\eta)$. Expanding $F(\eta,p)$ in Taylor's series with respect to p, we have

$$F(\eta,p) = f_0(\eta) + \sum_{k=1}^{+\infty} f_k(\eta)p^k = \sum_{k=0}^{+\infty}\phi_k(\eta)p^k, \tag{4.1.10}$$

where

$$f_k(\eta) = \frac{1}{k!}\frac{\partial^k F(\eta,p)}{\partial p^k}\Big|_{p=0}. \tag{4.1.11}$$

We define

$$\phi_0(\eta) = f_0(\eta), \tag{4.1.12}$$

$$\phi_k(\eta) = f_k(\eta) = \frac{1}{k!}\frac{\partial^k F(\eta,p)}{\partial p^k}\Big|_{p=0}, k \geqslant 1. \tag{4.1.13}$$

Differentiating the zero-order deformation Equation (4.1.4) m-times with respect to p and then dividing by $m!$ and finally setting $p = 0$ we get the following m-order deformation equation

$$\mathcal{L}\Big[\phi_m(\eta) - \chi_m\phi_{m-1}(\eta)\Big] = \hbar R_m(\phi_{m-1}(\eta)) = G_m(\eta), \quad m \geqslant 1 \tag{4.1.14}$$

where

$$R_m(\phi_{m-1}(\eta)) = \frac{1}{(m-1)!}\frac{\partial^{m-1}N[\phi(\eta)]}{\partial p^{m-1}}\bigg|_{p=0}. \tag{4.1.15}$$

• Let us try to find the general formula for $G_m(\eta)$

$$\begin{aligned}
&G_m(\eta) = \hbar R_m(\phi_{m-1}(\eta) = \hbar\Big\{\frac{1}{(m-1)!}\frac{\partial^{m-1}N[F(\eta,p)]}{\partial p^{m-1}}\bigg|_{p=0}\Big\}\\
&\Rightarrow G_m(\eta) = \hbar\Big\{\frac{1}{(m-1)!}\frac{\partial^{m-1}}{\partial p^{m-1}}\frac{\partial^3 F(\eta,p)}{\partial\eta^3} + F(\eta,p)\frac{\partial^2 F(\eta,p)}{\partial\eta^2} + \beta\Big[1-\Big(\frac{\partial F(\eta,p)}{\partial\eta}\Big)^2\Big]\Big\}\Big|_{p=0}\\
&\Rightarrow G_m(\eta) = \hbar\Big\{\frac{\partial^3}{\partial\eta^3}\Big[\frac{1}{(m-1)!}\frac{\partial^{m-1}F}{\partial p^{m-1}}\Big]_{p=0} + \Big[\frac{1}{(m-1)!}\frac{\partial^{m-1}}{\partial p^{m-1}}\Big[F\frac{\partial^2 F}{\partial\eta^2}\Big]\Big]_{p=0}\\
&\qquad\qquad + \beta\Big[\frac{1}{(m-1)!}\frac{\partial^{m-1}}{\partial p^{m-1}}\Big[1-\frac{\partial F}{\partial\eta}\frac{\partial F}{\partial\eta}\Big]\Big]_{p=0}\Big\}\\
&\Rightarrow G_m(\eta) = \hbar\Big\{\frac{\partial^3\phi_{m-1}}{\partial\eta^3} + \Big[\frac{1}{(m-1)!}\frac{\partial^{m-1}}{\partial p^{m-1}}\Big[F\frac{\partial^2 F}{\partial\eta^2}\Big]\Big]_{p=0} + \beta\Big[\frac{1}{(m-1)!}\frac{\partial^{m-1}}{\partial p^{m-1}}\Big[1-\frac{\partial F}{\partial\eta}\frac{\partial F}{\partial\eta}\Big]\Big]_{p=0}\Big\}.
\end{aligned}$$

• For $m=1$, we have

$$G_1(\eta) = \hbar\Big\{\frac{d^3\phi_0}{d\eta^3} + F(\eta,0)\frac{d^2F(\eta,0)}{d\eta^2} + \beta\Big[1-\frac{dF(\eta,0)}{d\eta}\frac{dF(\eta,0)}{d\eta}\Big]\Big\}.$$

Using (4.1.6), we can rewrite G_1 as

$$G_1(\eta) = \hbar\Big\{\frac{d^3\phi_0}{d\eta^3} + \phi_0\frac{d^2\phi_0}{d\eta^2} + \beta\Big[1-\frac{d\phi_0}{d\eta}\frac{d\phi_0}{d\eta}\Big]\Big\}. \tag{4.1.16}$$

• For $m=2$, we have

$$G_2(\eta) = \hbar\Big\{\frac{d^3\phi_1}{d\eta^3} + \sum_{k=0}^{1}\phi_k\frac{d^2\phi_{1-k}}{d\eta^2} - \beta\sum_{k=0}^{1}\frac{d\phi_k}{d\eta}\frac{d\phi_{1-k}}{d\eta}\Big\}. \tag{4.1.17}$$

• For $m=3$, we have

$$G_3(\eta) = \hbar\Big\{\frac{d^3\phi_2}{d\eta^3} + \sum_{k=0}^{2}\phi_k\frac{d^2\phi_{2-k}}{d\eta^2} - \beta\sum_{k=0}^{2}\frac{d\phi_k}{d\eta}\frac{d\phi_{2-k}}{d\eta}\Big\}. \tag{4.1.18}$$

According to (4.1.17) and (4.1.18), we can conjecture for the rest of the terms

• For m, we have

$$G_m(\eta) = \hbar\Big\{\frac{d^3\phi_{m-1}(\eta)}{d\eta^3} + \sum_{k=0}^{m-1}\phi_k(\eta)\frac{d^2\phi_{m-1-k}(\eta)}{d\eta^2} - \beta\sum_{k=0}^{m-1}\frac{d\phi_k(\eta)}{d\eta}\frac{d\phi_{m-1-k}(\eta)}{d\eta}\Big\}, \quad \text{for} \quad m\geqslant 2. \tag{4.1.19}$$

Let us use Equation (4.1.14) and try to express ϕ_m. We have

$$\begin{aligned}
&\mathcal{L}\Big[\phi_m(\eta) - \chi_m\phi_{m-1}(\eta)\Big] = \hbar R_m(\phi_{m-1}(\eta)) = G_m(\eta), \qquad m\geqslant 1\\
&\Rightarrow \phi_m - \chi_m\phi_{m-1} = \mathcal{L}^{-1}[G_m(\eta)]\\
&\Rightarrow \phi_m = \chi_m\phi_{m-1} + \mathcal{L}^{-1}[G_m(\eta)]
\end{aligned} \tag{4.1.20}$$

Liao (1999a) prove that (4.1.20) can be explicitly expressed in general form

$$\phi_m(\eta) = \sum_{k=0}^{m+1} \Psi_{m,k}(\eta) e^{-k\gamma\eta}, \quad m \geqslant 1; \tag{4.1.21}$$

where $\Psi_{m,k}(\eta)$ is defined by

$$\Psi_{0,0}(\eta) = b_{0,0}^0 + b_{0,0}^1 \eta, \tag{4.1.22}$$
$$\Psi_{0,1}(\eta) = b_{0,1}^0 + b_{0,1}^1 \eta, \tag{4.1.23}$$
$$\Psi_{m,0}(\eta) = b_{m,0}^0, \quad m \geqslant 1, \tag{4.1.24}$$
$$\Psi_{m,k}(\eta) = \sum_{i=0}^{2(m+1)-k} b_{m,k}^i \eta^i, \quad m \geqslant 1, \quad 1 \leqslant k \leqslant m+1, \tag{4.1.25}$$
$$b_{0,0}^0 = \frac{\omega}{\gamma^2} - \frac{1}{\gamma}, \tag{4.1.26}$$
$$b_{0,0}^1 = 1, \tag{4.1.27}$$
$$b_{0,1}^0 = -\frac{\omega}{\gamma^2} + \frac{1}{\gamma}, \tag{4.1.28}$$
$$b_{0,1}^1 = -\frac{\omega}{\gamma}. \tag{4.1.29}$$

Substituting (4.1.21) into (4.1.10) and setting $p = 1$, we obtain

$$\begin{aligned}
f(\eta) = F(\eta, 1) &= \sum_{m=0}^{M} \phi_m(\eta) \\
&= \sum_{m=0}^{M} \sum_{n=0}^{m+1} \Psi_{m,n}(\eta) e^{-n\gamma\eta} \\
&= \sum_{m=0}^{M} \Psi_{m,0}(\eta) + \sum_{m=0}^{M} \sum_{n=1}^{m+1} \Psi_{m,n}(\eta) e^{-n\gamma\eta} \\
&= \Psi_{0,0}(\eta) + \sum_{m=1}^{M} \Psi_{m,0}(\eta) + \sum_{m=0}^{M} \sum_{n=1}^{m+1} \Psi_{m,n}(\eta) e^{-n\gamma\eta} \\
&= b_{0,0}^0 + b_{0,0}^1 \eta + \sum_{m=1}^{M} \Psi_{m,0}(\eta) + \sum_{m=1}^{M} \sum_{n=1}^{m+1} \Psi_{m,n}(\eta) e^{-n\gamma\eta} + \sum_{n=1}^{1} \Psi_{0,n}(\eta) e^{-\gamma n\eta} \\
&= \eta + b_{0,0}^0 + \sum_{m=1}^{M} b_{m,0}^0 + \Psi_{0,1}(\eta) e^{-\gamma\eta} + \sum_{m=1}^{M} \sum_{n=1}^{m+1} \Psi_{m,n}(\eta) e^{-n\gamma\eta} \\
&= \eta + b_{0,0}^0 + \sum_{m=1}^{M} b_{m,0}^0 + \Psi_{0,1}(\eta) e^{-\gamma\eta} + \sum_{m=1}^{M} \sum_{n=1}^{m+1} \left(\sum_{k=0}^{2(m+1)-n} b_{m,n}^k \eta^k \right) e^{-n\gamma\eta} \\
&= \eta + \sum_{m=0}^{M} b_{m,0}^0 + \left(b_{0,1}^0 + b_{0,1\eta}^1 \right) e^{-\gamma\eta} + \sum_{m=1}^{M} \sum_{n=1}^{m+1} \left(\sum_{k=0}^{2(m+1)-n} b_{m,n}^k \eta^k \right) e^{-n\gamma\eta} \\
&= \eta + \sum_{m=0}^{M} b_{m,0}^0 + \sum_{m=0}^{M} \sum_{n=1}^{m+1} e^{-\gamma n\eta} \left(\sum_{k=0}^{2(m+1)-n} b_{m,n}^k \eta^k \right)
\end{aligned}$$

so, finally, we have

$$f(\eta) = \eta + \lim_{M\to\infty}\Big[\sum_{m=0}^{M} b_{m,0}^{0} + \sum_{m=0}^{M}\sum_{n=1}^{m+1} e^{-\gamma n\eta}\Big(\sum_{k=0}^{2(m+1)-n} b_{m,n}^{k}\eta^{k}\Big)\Big]. \tag{4.1.30}$$

The infinite sequences (4.1.30) gives a family of explicit analytical solutions in three parameters ω,$\gamma(\gamma > 0)$ and $\hbar(\hbar \neq 0)$.

4.1.2 Analytical solution.

In this case, we are working in the case of flow due to a line sink. Let us consider Equation (2.4.11)

$$\frac{d^3F}{dY^3} - \left(\frac{dF}{dY}\right)^2 + 1 = 0, \tag{2.4.11}$$

subject to the boundary conditions (2.4.12) and (2.4.13)

$$Y = 0,\ F = F' = 0 \tag{2.4.12}$$

$$Y \mapsto \infty, F' = 1 \text{ and } F'' = 0. \tag{2.4.13}$$

Our goal in this part is to find the exact solution of Equation (2.4.11). Multiplying Equation (2.4.11) by F'' and integrating after, we obtain

$$F''^2 = \frac{2}{3}\Big[(F')^3 - 3F' + 3C\Big], \tag{4.1.31}$$

where C is a constant to determine. Using the boundary condition (2.4.13), we have

$$\Big(F''(\infty)\Big)^2 = \frac{2}{3}\Big[(F'(\infty))^3 - 3F'(\infty) + 3C\Big] \Rightarrow C = \frac{2}{3}$$

and Equation (4.1.31) becomes

$$F''^2 = \frac{2}{3}\Big[(F')^3 - 3F' + 2\Big]. \tag{4.1.32}$$

We set

$$h(F') = (F')^3 - 3F' + 2, \tag{4.1.33}$$

where h is a function. we easily see that $h(1) = 0$ and the previous equation becomes

$$h(F') = \Big((F')^2 + F' - 2\Big)(F' - 1) = (F' - 1)^2(F' + 2). \tag{4.1.34}$$

Then Equation (4.1.32) becomes

$$\begin{aligned} F''^2 &= \frac{2}{3}\Big[(F' - 1)^2(F' + 2)\Big] \\ \Rightarrow F'' &= |\sqrt{\frac{2}{3}}\Big[(F' - 1)^2(F' + 2)\Big]^{\frac{1}{2}}| \\ \Rightarrow F'' &= \pm\sqrt{\frac{2}{3}}\Big[(F' - 1)^2(F' + 2)\Big]^{\frac{1}{2}}. \end{aligned} \tag{4.1.35}$$

We set for the next

$$F' = \theta \qquad \text{with} \qquad \theta = 0 \qquad \text{at} \qquad Y = 0, \tag{4.1.36}$$

and Equation (4.1.35) becomes

$$\theta' = \pm\sqrt{\frac{2}{3}}\Big[(\theta-1)(\theta+2)^{\frac{1}{2}}\Big] \iff \frac{d\theta}{dY} = \pm\sqrt{\frac{2}{3}}\Big[(\theta-1)(\theta+2)^{\frac{1}{2}}\Big] \Rightarrow Y = \mp\sqrt{2}\tanh^{-1}\left(\frac{\theta+2}{3}\right)^{\frac{1}{2}} + k.$$

Using the boundary condition

$$Y(0) = 0 \Rightarrow k = \pm\tanh^{-1}\left(\frac{2}{3}\right)^{\frac{1}{2}}$$

So,

$$Y = \mp\sqrt{2}\Big[\tanh^{-1}\left(\frac{\theta+2}{3}\right)^{\frac{1}{2}} \pm \tanh^{-1}\left(\frac{2}{3}\right)^{\frac{1}{2}}\Big]. \tag{4.1.37}$$

Let us now replace θ by F' and solve for F'. Replacing θ by F' in Equation (4.1.37), we have

$$Y = \mp\sqrt{2}\Big[\tanh^{-1}\left(\frac{F'+2}{3}\right)^{\frac{1}{2}} \pm \tanh^{-1}\left(\frac{2}{3}\right)^{\frac{1}{2}}\Big] \Rightarrow \mp\frac{Y}{\sqrt{2}} \mp \tanh^{-1}\left(\frac{2}{3}\right)^{\frac{1}{2}} = \tanh^{-1}\left(\frac{F'+2}{3}\right)^{\frac{1}{2}}.$$

After integrating we get

$$F = -3\sqrt{2}\tanh\left(\mp\frac{Y}{\sqrt{2}} \mp \tanh^{-1}\left(\frac{2}{3}\right)^{\frac{1}{2}}\right) + Y + A. \tag{4.1.38}$$

Using the boundary condition $F(0) = 0$, we find that $A = \mp 2\sqrt{3}$. So, finally the exact solution for a flow due to a line sink is

$$F = -3\sqrt{2}\tanh\left(\mp\frac{Y}{\sqrt{2}} \mp \tanh^{-1}\left(\frac{2}{3}\right)^{\frac{1}{2}}\right) + Y \mp 2\sqrt{3}. \tag{4.1.39}$$

4.2 Numerical solutions

4.2.1 SQLM applied to Falkner-Skan equations.

Let us consider the Falkner-Skan equations

$$N(\eta, f, f', f'', f''') \equiv \frac{d^3f}{d\eta^3} + f\frac{d^2f}{d\eta^2} + \beta\Big[1 - \left(\frac{df}{d\eta}\right)^2\Big] = 0, \tag{2.3.16}$$

subject to boundary conditions

$$\eta = 0,\ f = f' = 0 \tag{2.3.17}$$

and

$$\eta \mapsto \infty,\ f' = 1. \tag{2.3.18}$$

Let us solve this nonlinear equation using SQLM. We assume that the solution f_r at $(r+1)^{th}$ iteration are f_{r+1}. If the solution at the previous iteration are sufficiently close to the present iteration, the

nonlinear components of the Equation (2.3.16) can be linearised using Taylor's series. We have

$$N_r + \frac{\partial N_r}{\partial f_r'''}(f_{r+1}'''(\eta) - f_r'''(\eta)) + \frac{\partial N_r}{\partial f_r''}(f_{r+1}''(\eta) - f_r''(\eta)) + \frac{\partial N_r}{\partial f_r'}(f_{r+1}'(\eta) - f_r'(\eta)) + \frac{\partial N_r}{\partial f_r}(f_{r+1}(\eta) - f_r(\eta)) = 0$$
$$\Rightarrow \frac{\partial N_r}{\partial f_r'''}f_{r+1}''' + \frac{\partial N_r}{\partial f_r''}f_{r+1}'' + \frac{\partial N_r}{\partial f_r'}f_{r+1}' + \frac{\partial N_r}{\partial f_r}f_{r+1} = \frac{\partial N_r}{\partial f_r'''}f_r''' + \frac{\partial N_r}{\partial f_r''}f_r'' + \frac{\partial N_r}{\partial f_r'}f_r' + \frac{\partial N_r}{\partial f_r}f_r - N_r$$
$$\Rightarrow a_{0,r}f_{r+1}''' + a_{1,r}f_{r+1}'' + a_{2,r}f_{r+1}' + a_{3,r}f_{r+1} = a_{0,r}(\eta)f_r''' + a_{1,r}(\eta)f_r'' + a_{2,r}f_r' + a_{3,r}f_r - N_r$$
$$\Rightarrow a_{0,r}(\eta)f_{r+1}'''(\eta) + a_{1,r}(\eta)f_{r+1}''(\eta) + a_{2,r}(\eta)f_{r+1}'(\eta) + a_{3,r}(\eta)f_{r+1}(\eta) = R_r(\eta) \quad (4.2.1)$$

where

$$a_{0,r}(\eta) = \frac{\partial N}{\partial f_r'''} = 1 \quad (4.2.2) \qquad a_{1,r}(\eta) = \frac{\partial N}{\partial f_r''} = f_r \quad (4.2.3)$$

$$a_{2,r}(\eta) = \frac{\partial N}{\partial f_r'} = -2\beta f_r' \quad (4.2.4) \qquad a_{3,r}(\eta) = \frac{\partial N}{\partial f_r} = f_r'' \quad (4.2.5)$$

and

$$R_r(\eta) = a_{0,r}(\eta)f_r'''(\eta) + a_{1,r}(\eta)f_r''(\eta) + a_{2,r}(\eta)f_r'(\eta) + a_{3,r}(\eta)f_r(\eta) - N = -\beta(f_r')^2 + f_r''f_r - \beta. \quad (4.2.6)$$

The boundary condition in this case are

$$f_{r+1}(0) = 0, \quad (4.2.7)$$
$$f_{r+1}'(0) = 0, \quad (4.2.8)$$
$$f_{r+1}'(\infty) = 1. \quad (4.2.9)$$

Let us use the notion of spectral collocation method to simplify our equation (4.2.1).

The collocation process involves the evaluation of functions and their derivatives at selected grid points. Evaluating $\frac{df}{d\eta}$ at the grid points η_j gives

$$f'(\eta_j) = \sum_{k=0}^{N} D_{jk}f(\eta_k) = \mathbf{DF}, \quad j = 0, 1, 2, ..., N \quad (4.2.10)$$

at the Chebyshev-Gauss-Lobatto nodes

$$\eta_j = cos\frac{\pi j}{N}, \qquad j = 0, 1, 2...., N \quad (4.2.11)$$

where N+1 is the number of collocation points, **D** is the differentiation matrix and $\mathbf{F} = [f(x_0), f(x_1), ..., f(x_N)]^T$. So, we have

$$f_{r+1}'(\eta_j) = \mathbf{DF}_{r+1} \quad (4.2.12)$$

$$f_{r+1}''(\eta_j) = \Big(\mathbf{DF}_{r+1}\Big)' = \mathbf{D}\Big(\mathbf{DF}_{r+1}\Big) = \mathbf{D}^2\mathbf{F}_{r+1} \quad (4.2.13)$$

$$f'''_{r+1}(\eta_j) = \mathbf{D}^3\mathbf{F}_{r+1} \tag{4.2.14}$$

Substituting (4.2.12),(4.2.13) and (4.2.14) into (4.2.1), we have

$$\begin{aligned} & a_{0,r}(\eta_j)\mathbf{D}^3\mathbf{F}_{r+1} + a_{1,r}(\eta_j)\mathbf{D}^2\mathbf{F}_{r+1} + a_{2,r}(\eta_j)\mathbf{D}\mathbf{F}_{r+1} + a_{3,r}(\eta_j)\mathbf{F}_{r+1} = R_r(\eta_j) \\ & \Rightarrow \left(a_{0,r}\mathbf{D}^3 + a_{1,r}\mathbf{D}^2 + a_{2,r}\mathbf{D} + a_{3,r}\right)\mathbf{F}_{r+1} = \mathbf{R}_r \\ & \Rightarrow \mathbf{A}\mathbf{F}_{r+1} = \mathbf{R}_r \end{aligned} \tag{4.2.15}$$

where

$$\mathbf{A} = a_{0,r}\mathbf{D}^3 + a_{1,r}\mathbf{D}^2 + a_{2,r}\mathbf{D} + a_{3,r} \tag{4.2.16}$$

$$\mathbf{F}_{r+1} = [f_{r+1}(\eta_0), f_{r+1}(\eta_1), ..., f_{r+1}(\eta_N)]^T \tag{4.2.17}$$

$$\mathbf{R}_r = [R_r(\eta_0), R_r(\eta_1), ..., R_r(\eta_N)] \tag{4.2.18}$$

and $a_{p,r}$ are diagonal matrices

$$a_{p,r} = [a_{p,r}(\eta_0), a_{p,r}(\eta_1), ..., a_{p,r}(\eta_N)]^T \tag{4.2.19}$$

with the following boundary condition

$$f_{r+1}(\eta_N) = 0, \tag{4.2.20}$$

$$\sum_{k=0}^{N} D_{N,k} f_k = 0, \tag{4.2.21}$$

$$\sum_{k=0}^{N} D_{0,k} f_k = 1, \tag{4.2.22}$$

and we express (4.2.15) in vector form as

$$\begin{pmatrix} D_{0,0} & D_{0,1} & . & . & . & .D_{0,N} \\ A_{1,0} & A_{1,1} & . & . & . & A_{1,N} \\ A_{2,0} & A_{2,1} & . & . & . & A_{2,N} \\ . & & & & & \\ . & & & & & \\ A_{N-2,0} & A_{N-2,1} & & & & A_{N-2,N} \\ D_{N,0} & D_{N,1} & . & . & . & D_{N,N} \\ 0 & 0 & . & . & . & 1 \end{pmatrix} \begin{pmatrix} f(\eta_0) \\ f(\eta_1) \\ f(\eta_2) \\ . \\ . \\ f(\eta_{N-2}) \\ f(\eta_{N-1}) \\ f(\eta_N) \end{pmatrix} = \begin{pmatrix} 1 \\ R_r(\eta_1) \\ R_r(\eta_2) \\ . \\ . \\ R_r(\eta_{N-2}) \\ 0 \\ 0 \end{pmatrix} \tag{4.2.23}$$

Starting from a suitable initial guess $f_0(\eta)$ the approximate solution $f(\eta)$ can be obtained iteratively by solving equation (4.2.23) for r = 1, 2, 3,... We choose for our problem the initial guess which satisfy the above boundary condition

$$f_0(\eta) = \eta + e^{-\eta} - (1+\eta)e^{-\eta}. \tag{4.2.24}$$

4.2.2 ODE45 applied to Falkner-Skan equations.

Let us consider the Falkner-Skan equations

$$\frac{d^3f}{d\eta^3} + f\frac{d^2f}{d\eta^2} + \beta\left[1 - \left(\frac{df}{d\eta}\right)^2\right] = 0, \tag{2.3.16}$$

subject to boundary conditions

$$\eta = 0, \quad f = f' = 0 \tag{2.3.17}$$

and

$$\eta \mapsto \infty, \quad f' = 1. \tag{2.3.18}$$

To applied ODE45 to Equation (2.3.16), we should follow the following steps

• Transform the third-order nonlinear ODE (Falkner-Skan equations) into a system of first-order linear ODEs

• Transform our boundary value problem into an initial value problem by applying the shooting method.

A-Transform the third-order nonlinear ODE into a system of first-order linear ODEs

To be able to achieve that, let us set

$$\begin{cases} f(\eta) &= f_1 \\ f'(\eta) &= f_2 \\ f''(\eta) &= f_3 \end{cases} \Rightarrow \begin{cases} f_1' &= f_2 \\ f_2' &= f_3 \end{cases}$$

substituting into (2.3.16), we have

$$f_3' = -f_1 f_3 + \beta\left[f_2^2 - 1\right].$$

Finally, we have the following system of first-order linear ODEs

$$\begin{cases} f_1' &= f_2 \\ f_2' &= f_3 \\ f_3' &= -f_1 f_3 + \beta\left[f_2^2 - 1\right] \end{cases} \tag{4.2.25}$$

B-Transform boundary values problems into Initial values problems

According to Equation (4.2.25), we can rewrite the boundary conditions (2.3.17) and (2.3.18) as

$$\begin{cases} f_1(0) &= 0 \\ f_2(0) &= 0 \\ f_2(\infty) &= 1 \end{cases} \tag{4.2.26}$$

where $\eta = \infty$ is the unknown free boundary used to truncate the semi-infinite interval to a finite one which is to be determined as part of the procedure. To be able to use ODE45 to solve this equation, we

need a third initial condition. We set $f_3(0) = \alpha$ and we find the value of α which satisfy $f_2(\infty) = 1$. Equation (4.2.26) becomes

$$\begin{cases} f_1(0) &= 0 \\ f_2(0) &= 0 \\ f_3(0) &= \alpha \end{cases} \tag{4.2.27}$$

The solution of (4.2.25) and (4.2.27) depend on α. Denote $f_2(\infty) = \phi(\alpha)$ where $\phi(\alpha)$ ia a nonlinear function denoting the relation on how the value $f_2(\infty)$ depends on α. We need to find the value α such that $\phi(\alpha) = 1 \Rightarrow \phi(\alpha) - 1 = 0$.

Since $\phi(\alpha)$ is a nonlinear function, we need to find a root for the above nonlinear equation. To find that root, we need Newton's method or Secant method. For our case, we will use the Secant method because for Newton's method we need a derivative of our function and we do not have an expression of ϕ. For a Secant method, we just need 2 starting point α_1 and α_2. The algorithm for that goes as follows:

- Choose some initial guess α_1,α_2 and compute the values

$$\phi_1 = \phi(\alpha_1), \qquad \phi_2 = \phi(\alpha_2).$$

- Then, the next value α_3 could be completed by a secant step

$$\alpha_3 = \alpha_2 - \phi_2 \frac{\alpha_2 - \alpha_1}{\phi_2 - \phi_1}.$$

- Then, iterate and get values α_4, α_5,..., until converges. For example until $|\phi(\alpha_n) - 1| \leqslant$ tolerance.

4.3 Calculation of physical quantities

4.3.1 The shear stress.

In general, the shear stress value is calculated using this formula

$$\tau_w = \mu \left(\frac{\gamma + 1}{2}\right)^{\frac{1}{2}} \left(\frac{U^3}{\nu x}\right)^{\frac{1}{2}} f''(0). \tag{4.3.1}$$

Using the relation

$$\beta = \frac{2\gamma}{\gamma + 1} \tag{4.3.2}$$

and

$$\gamma = \frac{\beta}{2 - \beta} \tag{4.3.3}$$

and substituting into (4.3.1), we obtain

$$\tau_w = \frac{f''(0)}{\sqrt{2 - \beta}} \times \frac{1}{\sqrt{R_{ex}}} \rho U^2.$$

4.3.2 The friction coefficient.

In general, we have the following formula

$$C_f = \frac{\tau_w}{\frac{1}{2}\rho U^2} = \frac{\frac{f''(0)}{\sqrt{2 - \beta}} \times \frac{1}{\sqrt{R_{ex}}} \rho U^2}{\frac{1}{2}\rho U^2} = \frac{2}{\sqrt{2 - \beta}} \frac{f''(0)}{\sqrt{R_{ex}}}. \tag{4.3.4}$$

4.3.3 The Total friction force F or drag D.

$$F = \int_0^L \tau_w dx = \int_0^L \frac{f''(0)}{\sqrt{2-\beta}} \times \frac{1}{\sqrt{R_{ex}}} \rho U^2 = \frac{2f''(0)}{\sqrt{2-\beta}} \rho U^2 \left(\frac{\nu L}{U}\right)^{\frac{1}{2}}. \tag{4.3.5}$$

4.3.4 The displacement thickness.

In general, to compute the displacement thickness we use this formula

$$\delta = \int_0^\infty \left(1 - \frac{u}{U}\right) dy = \left(\frac{2}{m+1}\right)^{\frac{1}{2}} \left(\frac{\nu x}{U}\right)^{\frac{1}{2}} \int_0^\infty (1 - f'(\eta)) d\eta = (2-\beta)^{\frac{1}{2}} \left(\frac{\nu x}{U}\right)^{\frac{1}{2}} \int_0^\infty (1 - f'(\eta)) d\eta$$

$$\Rightarrow \delta(x) = \sqrt{2-\beta} \left(\frac{\nu x}{U}\right)^{\frac{1}{2}} \lim_{\eta \to \infty} [\eta - f(\eta)]. \tag{4.3.6}$$

5. Results and discussions

In this chapter, we present the results obtained using semi-analytic/analytical and numerical computation established in Chapter 4.

5.1 Semi-analytical result

The following computation has been made using MATHEMATICA software and we have obtained the following Table 5.1 and Figure 5.1.

β	HAM
-0.1988	-
0.0	0.4695
0.05	0.5310
0.1	0.5871
0.2	0.6869
0.3	0.7748
0.4	0.8544
0.5	0.9276
0.6	0.9957
0.8	1.1203
1.0	1.2327
1.2	1.3358
1.6	1.5215
2	1.6872

Table 5.1: Skin friction $f''(0)$ for different values of β using HAM,$\gamma = 5$,$\hbar = -1$ and $\omega = 0$.

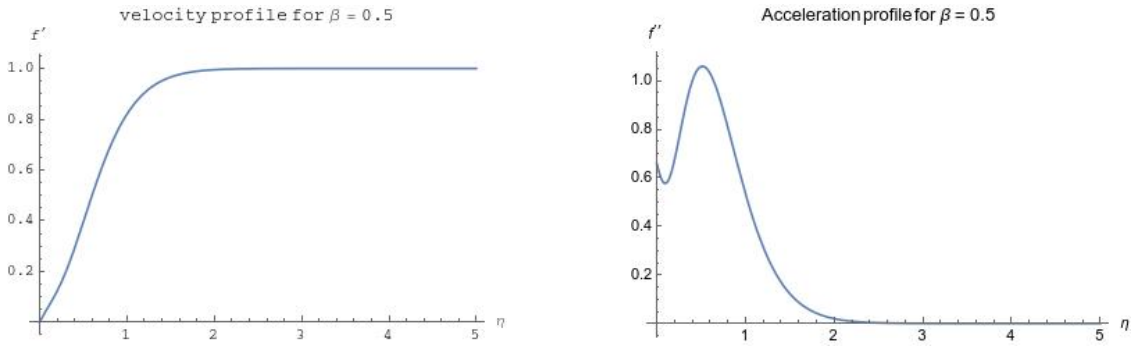

(a) Velocity profile.

(b) Acceleration profile.

Figure 5.1: Velocity and acceleration profile for $\beta = 0.5$ using HAM (3th order approximation).

The Table 5.1 gives us the value of the skin friction using HAM for certain values of β and suitable choice of auxiliary parameter $\hbar$ and integers γ,ω. The results started to converge after 20 order approximation i.e. M=20 in Equation (4.1.30). The Figure 5.1 shows us the velocity and acceleration profile of the solution of Falkner-Skan equations. We observe that the velocity and acceleration profile satisfy the boundary conditions of Falkner-Skan equations.

5.2 Numerical results

5.2.1 SQLM result.

The results here have been obtained using the MATLAB software. For the value of β, between $0 - 0.19884 \leqslant \beta \leqslant 2$ and $r = 10$ iterations, we obtain the following Table 5.2 and Figure 5.2.

β	SQLM	Residual error
-0.19884	0.00028052	7.42390286e-06
0.0	0.46959998	2.08022959e-08
0.05	0.53112963	3.96658852e-09
0.1	0.58703522	8.61234314e-09
0.2	0.68670818	2.13703945e-08
0.3	0.77475458	1.85009670e-08
0.4	0.85442123	2.74937113e-09
0.5	0.92768004	4.33912408e-09
0.6	0.99583644	1.10604120e-08
0.8	1.12026765	1.28968439e-08
1.0	1.23258765	7.29816513e-09
1.2	1.33572147	2.26264670e-08
1.6	1.52151399	2.11102958e-08
2.0	1.68721817	2.07669793e-08

Table 5.2: Skin friction $f''(0)$ for certain values of β and his residual error using SQLM.

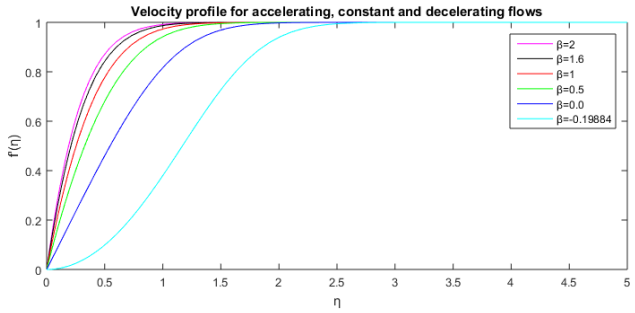

(a) Velocity profile $f'(\eta)$.

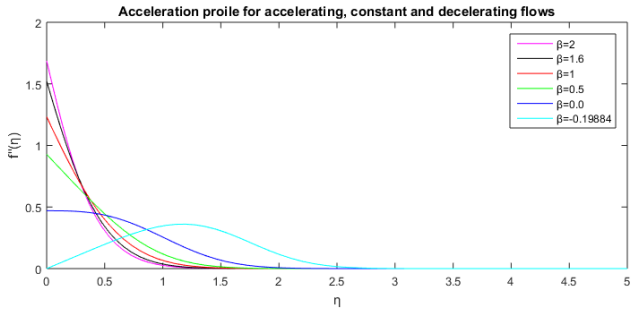

(b) Acceleration profile $f''(\eta)$.

Figure 5.2: Velocity and acceleration profile for β=-0.19884, 0, 0.5,1, 1.6 and 2 using SQLM

The Table 5.2 gives us the value of the skin friction and the residual error using SQLM for certain values

of β. The Figure 5.2 shows us the velocity and acceleration profile of the solution of Falkner-Skan equations. We observe that the velocity and acceleration profile satisfy the boundary conditions of Falkner-Skan equations. We also observe that, when β increases, the velocity profile become closer. This also applies the acceleration profile.

5.2.2 ODE45 result.

The results here were obtained using the MATLAB software. For the value of β, between $-0.19884 \leqslant \beta \leqslant 2$, we obtain the Table 5.3 and Figure 5.3.

β	ODE45
-0.19884	0.03988939
0.0	0.46964111
0.05	0.53114796
0.1	0.58704169
0.2	0.68670365
0.3	0.77474376
0.4	0.85440540
0.5	0.92765972
0.6	0.99585038
0.8	1.12026482
1.0	1.23257764
1.2	1.33570782
1.6	1.52184873
2	1.68756966

Table 5.3: Skin friction $f''(0)$ for certain value of β using ODE45.

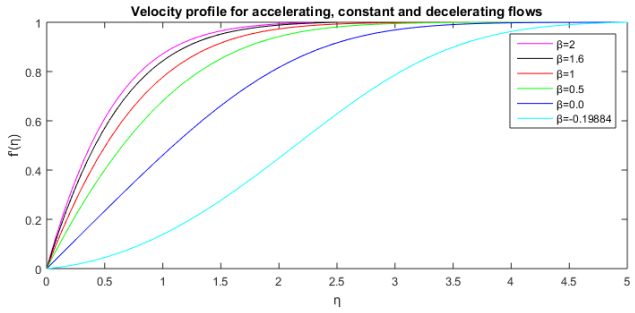

(a) Velocity profile $f'(\eta)$.

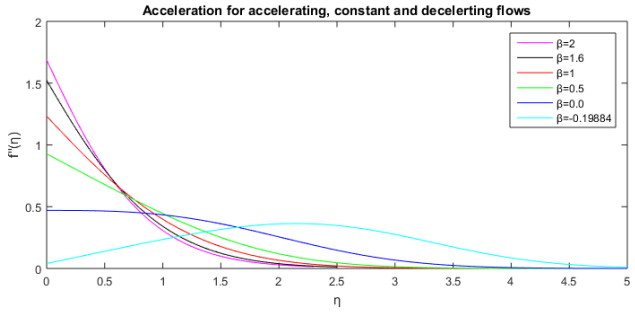

(b) Acceleration profile $f''(\eta)$.

Figure 5.3: Velocity and acceleration profile for β=-0.19884, 0, 0.5, 1, 1.6 and 2 using ODE45

The Table 5.3 gives us the value of the skin friction using ODE45 for certain values of β. The Figure 5.3 shows us the velocity and acceleration profile of the solution of Falkner-Skan equations. We observe that the velocity and acceleration profile satisfy the boundary conditions of Falkner-Skan equations. We also observe that, when β increases, the velocity profile become closer. This also applies the acceleration profile.

5.3 Comparison and discussion

5.3.1 HAM, SQLM and ODE45.

In Table 5.4, we present the skin friction value $f''(0)$ for different values of β using HAM, SQLM, ODE45 and compared to white (White, 1991). We also compute the iterative error for the numerical methods.

β	HAM	ODE45	SQLM	White (1991)
-0.19884	-	0.03988939	0.00028052	0.0
0.0	0.4695	0.46964111	0.46959998	0.4696
0.05	0.5310	0.53114796	0.53112963	0.5311
0.1	0.5871	0.58704169	0.58703522	0.5870
0.2	0.6869	0.68670365	0.68670818	0.6867
0.3	0.7748	0.77474376	0.77475458	0.7748
0.4	0.8544	0.85440540	0.85442123	0.8544
0.5	0.9276	0.92765972	0.92768004	0.9277
0.6	0.9957	0.99585038	0.99583644	0.9958
0.8	1.1203	1.12026482	1.12026765	1.1203
1.0	1.2327	1.23257764	1.23258765	1.2326
1.2	1.3358	1.33570782	1.33572147	1.3357
1.6	1.5215	1.52184873	1.52151399	1.5215
2	1.6872	1.68756966	1.68721817	1.6872

Table 5.4: Skin fiction comparisons between HAM, ODE45, SQLM and White (1991) for different value of β.

Number of iterations	$f''(0)$	iterative error for SQLM	$f''(0)$	iterative error for ODE 45
1	0.95443105	6.81111897e-02	-	-
2	0.92799880	1.33591361e-03	-	-
3	0.92768011	4.55812779e-07	1.10000000	1.74617354e-01
4	0.92768004	7.12514640e-09	0.92538265	2.35474442e-03
5	0.92768004	7.04520786e-09	0.92773739	7.76299831e-05
6	0.92768004	8.73602723e-10	0.92765976	4.20010117e-08
7	0.92768004	7.08559771e-09	0.92765972	7.67275132e-13
8	0.92768004	1.23886963e-08	0.92765972	2.22044605e-16
9	0.92768004	6.44179432e-09	-	-
10	0.92768004	2.03176874e-09	-	-

Table 5.5: Comparisons between number of iterations and the iterative error for $\beta = 0.5$.

β	10th-order	15th-order	20th-order
0.5	0.9338	0.9280	0.9276

Table 5.6: Order of convergence for skin friction $f''(0)$ using HAM for $\beta = 0.5$.

β	time for SQLM (s)	time for ODE45(s)	time for HAM (min)
0.0	0.025418	0.373065	many minutes
1.0	0.017325	0.494817	many minutes
2.0	0.019390	0.545128	many minutes

Table 5.7: Time comparison for all the methods to converges to solution.

From Table 5.5, we remark that the SQLM method starts to converge at iteration number 4 while the ODE45 start converging at iteration number 7. We also see that the iterative error of SQLM method at iteration number 3 is 10^{-7} while the iterative error for ODE45 at the same number of iterations is just 10^{-1}. We conclude that the SQLM method is more accurate than the ODE45 method and follow by HAM because HAM converges after 20^{th} order approximation (see Table 5.6).

Concerning the efficiency of the methods, the results indicate that the time taking to converges for ODE45 is around the order 10^{-1} seconds while time taking to converge using SQLM is around 10^{-2} seconds (see Table 5.7). The HAM is about many minutes. So we conclude that SQLM is more efficient compared to ODE45 and HAM.

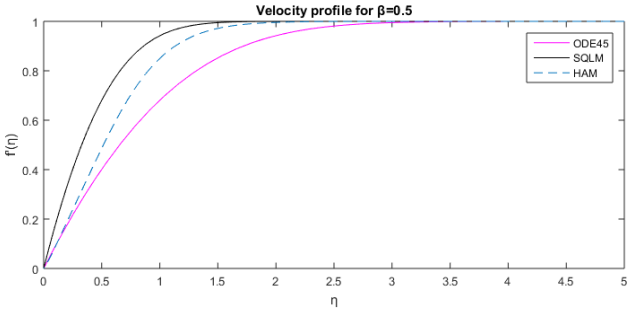

(a) Velocity profile.

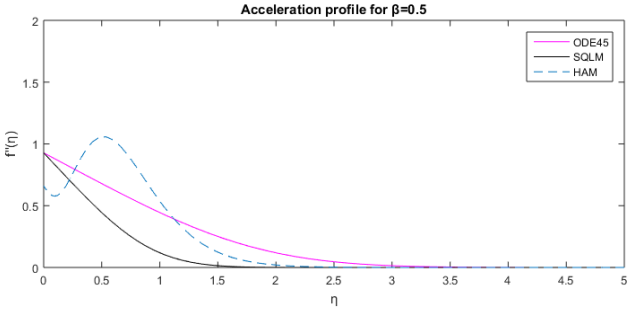

(b) Acceleration profile.

Figure 5.4: Velocity and acceleration comparison between HAM (3th order approximation), ODE45 and SQLM for $\beta = 0.5$.

The Figure 5.4 shows us the comparison between the velocity and acceleration profile for the HAM,

SQLM and ODE45. We observe that the HAM is not enough smooth compare to SQLM and ODE45.

5.3.2 Exact solution and SQLM.

Iteration	$f''(0)$	SQLM residual error
1	1.18778312	2.15845032e-01
2	1.15201251	1.59612518e-03
3	1.15178724	9.78669856e-08
4	1.15178723	1.96914042e-10
5	1.15178723	2.29946055e-10
6	1.15178723	6.62348162e-10
7	1.15178723	2.12295524e-10
8	1.15178723	3.21155702e-10
9	1.15178723	4.33530109e-10
10	1.15178723	2.73977155e-10

Table 5.8: Skin friction for a flow due to a line sink and his corresponding residual error using SQLM

In case of a flow due to a line sink, we found the exact solution of equation (2.4.11) and the exact solution of the skin friction, in this case, is 1.1547. Using SQLM, we obtain the value of skin friction 1.15178723 (see Table 5.8) which is not bad if we look at the residual error which is around 10^{-10}. So SQLM method is a very good method to approximate the solution in the case of flow due to a line sink. We can also look at the velocity profile and acceleration profile and see that they have the same shape (see Figure 5.5).

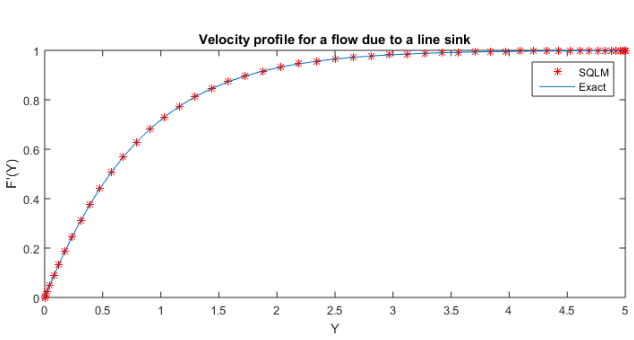

(a) velocity profile.

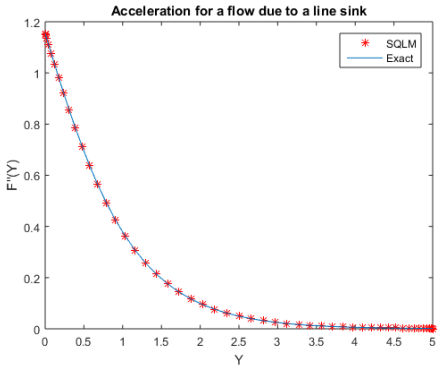

(b) Acceleration profile.

Figure 5.5: Velocity and acceleration profile for exact and approximate solution

5.3.3 Physical interpretation.

The skin friction is a resistant force exerted on an object moving in a fluid. The skin friction is caused by the viscosity of fluids and developed when a fluid moves on the surface of an object.

The shear stress is defined as a force per unit area, acting parallel to an infinitesimal surface element. The shear stress in a fluid is a measure of the resistance to the fluid movement and is related to the fluid viscosity.

• When $\beta > 0$, we are in the case of favourable pressure gradient $(\frac{\partial p}{\partial x} < 0)$ on the boundary layer. Here the skin friction increases when β increases. Consequently, the resistant force exerted on an object

moving in a fluid, the shear stress, the friction coefficient, and the drag force also increase. But the displacement thickness decrease in this case.

• When $\beta < 0$, we are on the case of adverse pressure gradient $(\frac{\partial p}{\partial x} < 0)$ on the boundary layer. Here the skin friction reduces with β (when β decreases, the resistant force exerted on an object also decreases). Consequently, the shear stress, the friction coefficient, and the drag force also decrease. But the displacement thickness increase in this case. But there is a limit when $\beta = -0.19884$.

– When $\beta = -0.19884$, we are in the case where the skin friction is almost zero i.e. there is no resistant force i.e. no viscosity. Consequently, the shear stress, the friction coefficient, and the drag force are all equal to zero. Note that this case is the case where the displacement thickness is larger. This value of β correspond to the angle 18 degree.

β	$\frac{\tau_w}{\rho U^2} \times \sqrt{R_{ex}}$	$C_f \times \sqrt{R_{ex}}$	$F \times \frac{1}{\rho U^2 \left(\frac{\nu L}{U}\right)^{\frac{1}{2}}}$
-0.1988	0.0002	0.0004	0.0004
0.0	0.33205733	0.664114661	0.664114661
1.0	1.23258765	2.4651753	2.4651753
1.6	2.40572485	4.8114497	4.8114497

Table 5.9: Values of τ_w , C_f and F for certain value of β using $f''(0)$ arising from SQLM

β	δ_x
-0.1988	$\sqrt{2.199}\left(\frac{\nu x}{U}\right)^{\frac{1}{2}} \lim_{\eta\to\infty}[\eta - f(\eta)]$
0.0	$\sqrt{2}\left(\frac{\nu x}{U}\right)^{\frac{1}{2}} \lim_{\eta\to\infty}[\eta - f(\eta)]$
1.0	$\left(\frac{\nu x}{U}\right)^{\frac{1}{2}} \lim_{\eta\to\infty}[\eta - f(\eta)]$
1.6	$\sqrt{0.4}\left(\frac{\nu x}{U}\right)^{\frac{1}{2}} \lim_{\eta\to\infty}[\eta - f(\eta)]$

Table 5.10: δ_x for certain value of β using $f''(0)$ arising from SQLM

6. Conclusion and future work

6.1 Conclusion

Our goal in this work was to compare semi-analytical and numerical methods for solving Falkner-Skan equations and determine physical quantities such as skin friction, shear stress, friction coefficient, total friction force, and displacement. Our objectives included the derivation of the Falkner-Skan equations starting from Navier-Stokes equations; analyse the equations for stagnation point flow, flow past a wedge, flow past a flat plate, flow around a corner and flow due to a line sink; find the semi-analytical solution of the Falkner-Skan equations using homotopy analysis method (HAM); find numerical solution using spectral quasi-linearisation method (SQLM) and ODE45; compare the analytical and numerical solutions; compute and explain the following parameters for certain types of fluid flow: skin friction, shear stress, friction coefficient, friction force, and displacement thickness.

This study shows that, the numerical method SQLM which converges after 4 iterations, iterative error of order 10^{-7} after 3 iterations, time to converge to the solution around 10^{-2} second is more accurate and efficient than ODE45 which converges after 7 iterations, iterative error of order 10^{-1} after 3 iterations, time to converge to the solution around 10^{-1} second and the semi-analytical method HAM which converges after 20 order approximation, times to converge to the solution many minutes. They also help us to see that all our numerical methods were more accurate and efficient than the semi-analytical methods. Concerning the case where we obtain the exact solution (flow due to a line sink), we observe that the SQLM method approximates well the exact solution with the residual error around 10^{-10}.

Another aspect of this work was to determine physical quantities such as skin friction, shear stress, friction coefficient, total friction force, and displacement thickness depending on a dimensionless pressure gradient parameter β. We observed that when $\beta > 0$, which correspond to the case of favourable pressure gradient ($\frac{\partial p}{\partial x} > 0$) the skin friction increases when β increases. Consequently, the resistant force exerted on an object moving in a fluid, the shear stress, the friction coefficient, and the drag force also increase. But the displacement thickness decrease in this case. When $\beta < 0$, which correspond to the case of adverse pressure gradient ($\frac{\partial p}{\partial x} < 0$) the skin friction reduces when β reduce. Consequently, the shear stress, the friction coefficient, and the drag force also decrease. But the displacement thickness increase in this case. We also observe that in this case of adverse pressure gradient when $\beta = -0.19884$, we are in the case where the skin friction is almost zero which implies that there is no resistant force ie no viscosity and consequently, the shear stress, the friction coefficient, and the drag force are all equal to zero. This case is the case where the displacement thickness is larger and the corresponding angle is 18 degree.

6.2 Future work

This subject was exciting to study, but we were limited by the time allowed to submit the thesis. One of the potential future studies will be to use other powerful numerical methods such as the finite element method or Keller Box method. Also, we can consider the case of the turbulent boundary layer and observe how the physical quantities behave.

Acknowledgements

First of all, thanks to the almighty God for everything he has done in my life.

I want to express my most profound feeling of gratitude toward Prof. Precious Sibanda, my supervisor, and Dr. Sicelo Goqo, my co-supervisor, for their valuable guidance and continuous support. They have been such wonderful supervisors, and I am infinitely grateful.

I also thanks AIMS, and it's funders for supporting this work.

Special profound gratitude to the following people: Prof. Barry Green(AIMS Director) Dr. Simukai Utete (Academic director), Prof. J.W Sanders, Jan Groenewald (IT manager), and my tutors Prudence, Rock, Lebeko, Jordan, Taboka, Leila, Kenneth, Bachir...

Thanks to my English teacher, the unique and special, Noluvuyo Hobana.

Special thanks should be given to my new family, my fraternity, Lebogang, Kiprono, Saumu, Tshenolo, Mzwake, Star, Zainab, Ghislaine, Willy, William, Alex, Blessing, Zizipho, Alungile, Katlego, Kibidi, Karabo , Menzi and all AIMS students.

Finally, I wish to thanks my parents, Mr. and Mrs. NKOCKO, my sisters NKOCKO DONFACK careme Larissa, NKOCKO AWOUAFACK loriane ingrid, KADJOU NKOCKO jovine hornella, my brothers NKOCKO DJOUKANG rayan fred, SONFACK TCHAGNAN audrey kevin and my niece LEKANE NGOUFACK TAZANO euclide.

References

Asaithambi, N. A numerical method for the solution of the falkner-skan equation. *Applied Mathematics and Computation*, 81(2-3):259–264, 1997.

Barania, H., Haghparast, N., Miansari, M., and Barari, A. Flow analysis for the falkner–sken wedge flow. *Current Science* 69–177, 2012.

Blasius, H. Grenzschichten in flüssigkeiten mit kleiner reibung. *Z. Angew. Math. Phys. 56* 1–37, 1908.

Duque-Daza, C., Lockerby, D., and Galeano, C. Numerical solution of the falkner-skan equation using third-order and high-order-compact finite difference schemes. *Journal of the Brazilian Society of Mechanical Sciences and Engineering*, 33(4):381–392, 2011.

Hartree, D. R. On an equation occurring in falkner and skan's approximate treatment of the equations of the boundary layer. In *Mathematical Proceedings of the Cambridge Philosophical Society*, volume 33 223–239, 1937.

He, J.-H. A simple perturbation approach to blasius equation. *Applied Mathematics and Computation*, 140(2-3):217–222, 2003.

Ishak, A., Nazar, R., and Pop, I. Falkner-skan equation for flow past a moving wedge with suction or injection. *Journal of Applied Mathematics and Computing*, 25(1-2):67–83, 2007.

Liao, S. An explicit totally analytic approximation of blasius viscous flow problems. *International Journal of Nonlinear Mechanics*, 34:759–778, 1999a.

Liao, S.-J. *The proposed homotopy analysis technique for the solution of nonlinear problems*. PhD thesis, Shanghai Jiao Tong University Shanghai, 1992.

Liao, S.-J. A uniformly valid analytic solution of two-dimensional viscous flow over a semi-infinite flat plate. *Journal of Fluid Mechanics*, 385:101–128, 1999b.

MacKay, D. A free energy minimization framework for inference problems in modulo 2 arithmetic. In Preneel, B., editor, *Fast Software Encryption (Proceedings of 1994 K.U. Leuven Workshop on Cryptographic Algorithms)*, Lecture Notes in Computer Science Series 179–195, 1995.

Marinca, V., Ene, R.-D., and Marinca, B. Analytic approximate solution for falkner-skan equation. *The Scientific World Journal*, 2014, 2014.

Moallemi, N., Shafieenejad, I., Hashemi, S., and Fata, A. Approximate explicit solution of falkner-skan equation by homotopy perturbation method. *Res. J. Appl. Sci. Eng. Technol*, 4(17):2893–2897, 2012.

nptel. Laminar boundary layers. nptel, https://nptel.ac.in/content/storage2/courses/112104118/lecture-28/28-2_boundary_eq.htm, Accessed October, 19 2019.

Parand, K., Pakniat, N., and Delafkar, Z. Numerical solution of the falkner-skan equation with stretching boundary by collocation method. *International Journal of Nonlinear Science*, 11(3):275–283, 2011.

Parveen, S. Numerical solution of the falkner skan equation by using shooting techniques. *IOSR Journal of Mathematics*, 10(2-3):78–83, 2014.

Prandtl, L. Über flussigkeitsbewegung bei sehr kleiner reibung. *Verhandl. III, Internat. Math.-Kong., Heidelberg, Teubner, Leipzig, 1904* 484–491, 1904.

VM, F. and SW, S. Some approximate solutions of the boundary-layer for flow past a stretching boundary. *SIAM J Appl Math*, 49:1350–1358, 1931.

White, F. Solutions of the newtonian viscous flow equations. *Viscous Fluid Flow* 104–217, 1991.

White, F. M. and Corfield, I. *Viscous fluid flow*, volume 3. McGraw-Hill New York, 2006.

Wikipedia. Boundary layer. Wikipedia, the Free Encyclopedia, https://en.wikipedia.org/wiki/Boundary_layer, Accessed October,19 2019.

Zhu, S., Wu, Q., and Cheng, X. Numerical solution of the falkner–skan equation based on quasilinearization. *Applied Mathematics and Computation*, 215(7):2472–2485, 2009.